Invited review paper submitted to Journal of Structural Geology, March 29, 2020

Folding and fracturing of rocks adjacent to salt diapirs

***Mark G. Rowan[1], Josep Anton Muñoz[2], Katherine A. Giles[3], Eduard Roca[2], Thomas E. Hearon IV[4], J. Carl Fiduk[5], Oriol Ferrer[2], Mark P. Fischer[6]**

[1] Rowan Consulting, Inc., 850 8th St., Boulder, CO 80302, USA mgrowan@frii.com 1.303.545.9437
[2] Institut de Recerca Geomodels, Departament de Dinàmica de la Terra i de l'Oceà, Universitat de Barcelona, Barcelona, Spain jamunoz@ub.edu eduardroca@ub.edu joferrer@ub.edu
[3] Institute of Tectonic Studies, Department of Geological Sciences, The University of Texas at El Paso, 500 W. University, El Paso, TX 79902, USA kagiles@utep.edu
[4] EOG Resources, 600 17th St., Suite 1000N, Denver, CO 80202, USA thomashearon@gmail.com
[5] Fiduk Consulting LLC, 9593 Doliver Dr., Houston, TX 77063, USA fidukjc@yahoo.com
[6] Department of Geology and Environmental Geosciences, Northern Illinois University, 1425 W. Lincoln Hwy., De Kalb, IL 60115, USA mfischer@niu.edu

Keywords

Salt diapir; Salt sheet; Folds; Faults; Fractures; Shear

Abstract

This review paper examines deformation adjacent to salt stocks and walls and beneath salt sheets, with a focus on passive salt rise or emplacement and structures ranging from large-scale folds and faults to small-scale folds, fractures, and shear zones. The analysis begins with a summary of the existing literature on analog and numerical modeling and empirical subsurface and outcrop data, which offer conflicting interpretations and models. The emphasis here, however, is on exposed diapirs and sheets in a variety of salt basins. These demonstrate that near-salt deformation during passive diapirism is less common and less pronounced than is typically thought. In most cases, diapir rise and sheet emplacement do not directly shear and fracture adjacent strata. Instead, salt movement leads to drape folding of a thin roof, which in turn may cause associated fracturing, just as with folding of any origin. There can be exceptions, with the most common being regional extensional, contractional, or strike-slip deformation that is coeval with or postdates diapirism. This is especially the case if the salt becomes welded and there is ongoing weld-parallel slip or if fault damage zones formed away from diapirs subsequently become juxtaposed against the salt.

1. Introduction

Salt structures involve flow of ductile salt with respect to surrounding sedimentary rocks, which normally deform as frictional materials. In those with concordant overburden, such as salt pillows or salt-cored anticlines, strata just above the top salt display no increase in deformation compared to regional, background levels. Yet flow of salt with a discordant relationship with younger strata (i.e., diapiric salt; Hudec and Jackson, 2011), whether more vertically in salt stocks and salt walls or more laterally in salt sheets, is commonly thought to have caused significant deformation of adjacent rocks (Fig. 1). The idea of folding, fracturing, and shearing of surrounding strata due to salt emplacement has been promulgated for decades. Seventy-five years ago, Wallace (1944, p. 1305) stated that "…salt movement caused the sediments to be faulted or sheared by the salt." Twenty-four years later, Murray (1968) reiterated that "…piercement of the enclosing strata has been accompanied by varying degrees of up-warping and thinning of the adjacent beds" (p. 109), adding that "…shale sheath … is very similar in texture to fault gouge, … formed by … fragmentation during growth of the salt stock" (p. 112). Over two decades later, Jackson and Talbot (1991, p. 11) defined an external shear zone (also termed a drag zone) as a sheath-like collar around the diapir due to contact strain, with its outer part comprising "a ductile shear zone, a brittle shear zone, a fault, or a growth fault" depending on the rheology of the overburden. Similarly, Harrison and Patton (1995, p. 104) applied the same concept to salt sheets, interpreting "shear zones localized at or just below the salt" (Fig. 1a). At the beginning of this century, Alsop et al. (2000, p. 1019) noted that rotations of diapir-flanking strata "are associated with significant attenuation and folding of the overburden, coupled with marked faulting and fracturing" (Figs. 1b, c). And in their recent textbook, Jackson and Hudec (2017) depicted the presence of fracture halos around diapirs (p. 433) (Fig. 1d) and shear zones adjacent to diapirs and beneath salt sheets (p. 451).

Yet throughout the same period, there have been dissenting observations, interpretations, and opinions. Parker and McDowell (1955) postulated that at least some of the stratal thinning over diapirs was depositional and that folding was caused by doming and penetration of a roof. Bornhauser (1969, p. 1411) mentioned that some diapirs have "very little or no drag", and Kolarsky (1996) reported a notable lack of faulting around one Gulf of Mexico salt dome, reinterpreting surfaces representing missing stratigraphy as unconformities instead of faults. More recently, field exposures of both small- and large-scale near-diapir folding have been used to demonstrate that bed thinning is depositional, not structural, and that faulting/fracturing is minimal (Rowan et al., 2003, 2016), and Hearon et al. (2015a) observed no shear zones or thrust faults beneath exposed salt sheets in South Australia.

The primary goal of this paper is to investigate these apparently contradictory claims. Does diapiric salt, i.e. salt that has 'pierced' overlying strata, have any greater impact on the deformation of adjacent sediments than salt that is conformable with its overburden? What is the nature and origin of any near-diapir deformation, and why do some diapirs appear to have considerably more flanking deformation than others? We approach the topic with an emphasis on

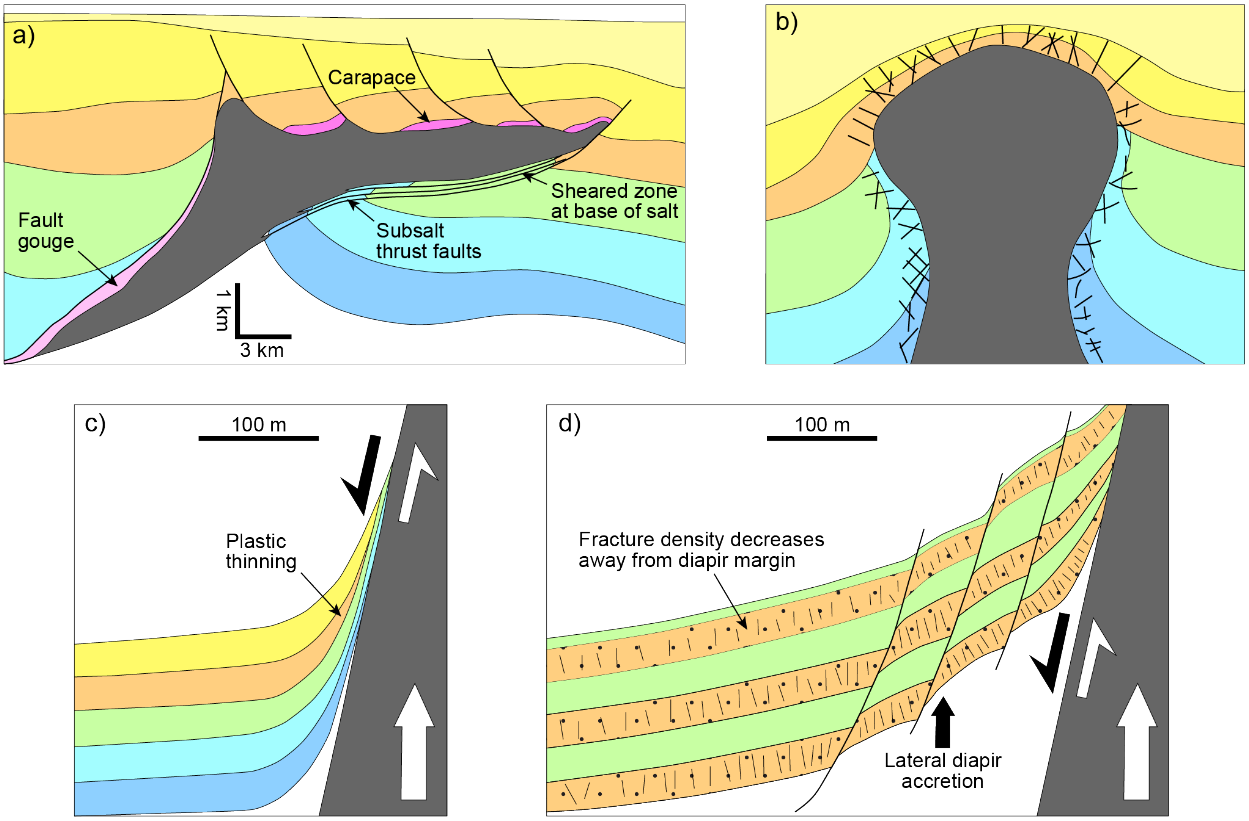

***Figure 1**. Interpretations of near-diapir deformation: a) salt sheet with suprasalt fault gouge and subsalt thrust faults and shear zone (modified from Harrison and Patton, 1995); b) fracture halo due to diapir rise (no scale; modified from Jackson and Hudec, 2017); c) narrow, pronounced drag zone of structurally thinned homogeneous incompetent layers (modified from Alsop et al., 2000); d) broad, segmented drag zone of heterogeneous competent overburden (orange – sandstones, green – shales and coals) (modified from Alsop et al., 2000).*

outcrop evidence – what do we see and what don't we see adjacent to exposed salt stocks/walls and beneath exposed salt sheets? We also incorporate subsurface data where relevant, but with the caveat that seismic data have limited resolution and wells provide only one-dimensional samples, and we compare field observations to the results of analog and numerical models.

One of the primary difficulties when dealing with deformation patterns around salt structures is distinguishing between structures resulting from regional stress and those related to salt flow itself. Because salt is the weakest sedimentary rock at upper crustal levels, any tectonic event will result in the localization of strain in the diapirs and sheets that may thus impact adjacent rocks. As a consequence, we may expect overprinting by syn- or post-diapiric regional deformation.

Salt diapirs include such features as triangular salt rollers in the footwalls of extensional faults and slivers of salt carried up in the hanging walls of thrust faults. The focus here, though, is on passive diapirs, i.e., those growing at or just beneath the ground surface or sea floor concurrently with sedimentation (Hudec and Jackson, 2011; Jackson and Hudec, 2017). This includes steep salt stocks and salt walls as well as many lower-angle allochthonous salt sheets. Note that we refer in this paper to passive diapirism *sensu lato*, i.e., ongoing near-surface growth regardless of whether the salt crest is exposed (passive diapirism *sensu stricto*) or buried beneath a thin, folded and uplifted roof (active diapirism *sensu stricto*) (see Jackson et al., 1988; Schultz-Ela et al., 1993; Rowan et al., 2003; Jackson and Hudec, 2017; Rowan and Giles, 2020). Also, in the case of salt sheets, we focus more on near-salt deformation beneath and in front of the advancing sheet, not on the evolution of its roof, which is dominated by subsidence into the salt and/or gravity-driven extension and contraction.

In the sections below, we first summarize the rheology of evaporites and their surrounding strata. We then review the published literature, addressing firstly numerical and experimental models and secondly empirical data from the subsurface (seismic images and well bores) and outcrops. In the main body of the paper, we offer our own thoughts, using primarily exposed salt structures, including both steep stocks/walls and low-angle salt sheets, to evaluate folding, fracturing, and shearing of strata near salt. We conclude that: 1) salt-induced shear and associated fracturing is largely absent; 2) stratal thinning is primarily depositional rather than structural; 3) folding is due to drape of a roof over the edge of rising or advancing salt rather than to frictional drag; and 4) local faults/fractures do exist but are related primarily to fold development or regional deformation, not salt flow *sensu stricto*. We emphasize deformation attributed directly to salt emplacement, with relatively minor discussion of that due to regional tectonics (extension or shortening, whether coeval with or subsequent to salt emplacement), minibasin-scale salt evacuation, hydraulic fracturing, or local dissolution of salt. Moreover, we distinguish between structural/tectonic deformation, which is the focus of this paper, and soft-sediment deformation, which we consider to be a depositional process. Note that we do not address, except in passing, such possible effects of diapirism on near-diapir variations in pore pressure, compaction and cementation, or fluid flow and alteration.

2. Rheology of salt and adjacent strata

In order to properly assess modeled and observed near-diapir deformation, it is critical to understand the contrast in rheology between diapirs and their adjacent strata. Thus, we summarize below the strength and deformation mechanisms of typical rocks within and around diapirs.

Diapirs are made up of layered evaporite sequences and thus comprise variable percentages of halite, anhydrite, gypsum, bittern salts, and non-evaporite components such as carbonates, siliciclastics, and volcanic and shallow intrusive rocks (e.g., Warren, 2016; Jackson and Hudec, 2017; Rowan et al., 2019b). (Note that in the remainder of the paper, we use the term ‘salt’ to refer to the entire deformed layered evaporite sequence regardless of the proportions of halite and other lithologies or whether the halite has been dissolved to form caprock.) In diapirism, thicker strong layers tend to get disrupted and form a mélange of stringers in a matrix of complexly folded halite, minor bittern salts, and thin anhydrite or shale interlayers (Rowan et al., 2019b). Halite, as the dominant mineral, is weak and ductile and thus best viewed as a power-law fluid that creeps under differential stress typically between 0.5 and 2 MPa (e.g., Spiers and Carter, 1998; Schléder and Urai, 2005, 2007; Urai et al., 2008). The effective viscosities at these differential stresses are 10^{18} to 10^{19} Pa s.

In contrast, surrounding strata (siliciclastic and carbonate rocks) are significantly stronger Mohr-Coulomb materials that deform according to frictional-plastic constitutive laws (e.g., Weijermars et al., 1993). The strength can vary depending on the lithology, the mechanical stratigraphy of the multilayer, the depth of burial, the amount of overpressure, and the strain rate. Moreover, frictional-plastic materials are weaker during extension than during contraction, deforming readily by brittle fracturing.

The rheological contrast between diapirs and their surrounding strata (at uppermost crustal levels) results in the salt flowing as a viscous material between or above strong bounding sedimentary rocks (see Jackson and Hudec, 2017, section 3.5). This creates viscous (or boundary) drag within the salt. In Poiseuille flow, there is theoretically zero flow or slip at the edge of the salt, with a zone of internal shear just inside the margins accommodating movement of the center of the salt body relative to its boundaries (Fig. 2a). Similarly, there is no slip at the salt boundaries in Couette flow (Fig. 2b). This is well exposed in the Sierra Madre Oriental of northern Mexico, where the autochthonous salt layer (gypsum in this case) is the detachment in a thin-skinned fold-and-thrust belt. Starting beneath the salt and moving up into the gypsum, we see: 1) undeformed redbeds; 2) a 10 m thick zone of undeformed gypsum with preserved early diagenetic chicken-wire texture; 3) a zone 5-10 m thick of upwardly increasing development of a planar fabric; and 4) a mylonitic shear zone (Fig. 2c; Cross, 2012). In other words, the detachment is not the base-salt surface but an internal shear zone near the base. Presumably, the main zone of shear would be closer to the boundary in lower-viscosity halite. Schematic representations of salt flow in a vertical diapir and a salt sheet are shown in Figures 2d and 2e, respectively, although these do not take into account any intrasalt heterogeneity.

3. Literature review

In the following sections, we review much of the extensive literature on diapir-related deformation. We split this into two parts: first, the results of experimental, numerical, and analytical models; and second, interpretations of subsurface and surface empirical data. In both cases, we address first steep salt stocks and walls and then low-angle salt sheets. Again, the focus is on deformation associated with diapir growth and salt-sheet emplacement and advance, not superimposed regional deformation, although admittedly these cannot always be distinguished (see Discussion section).

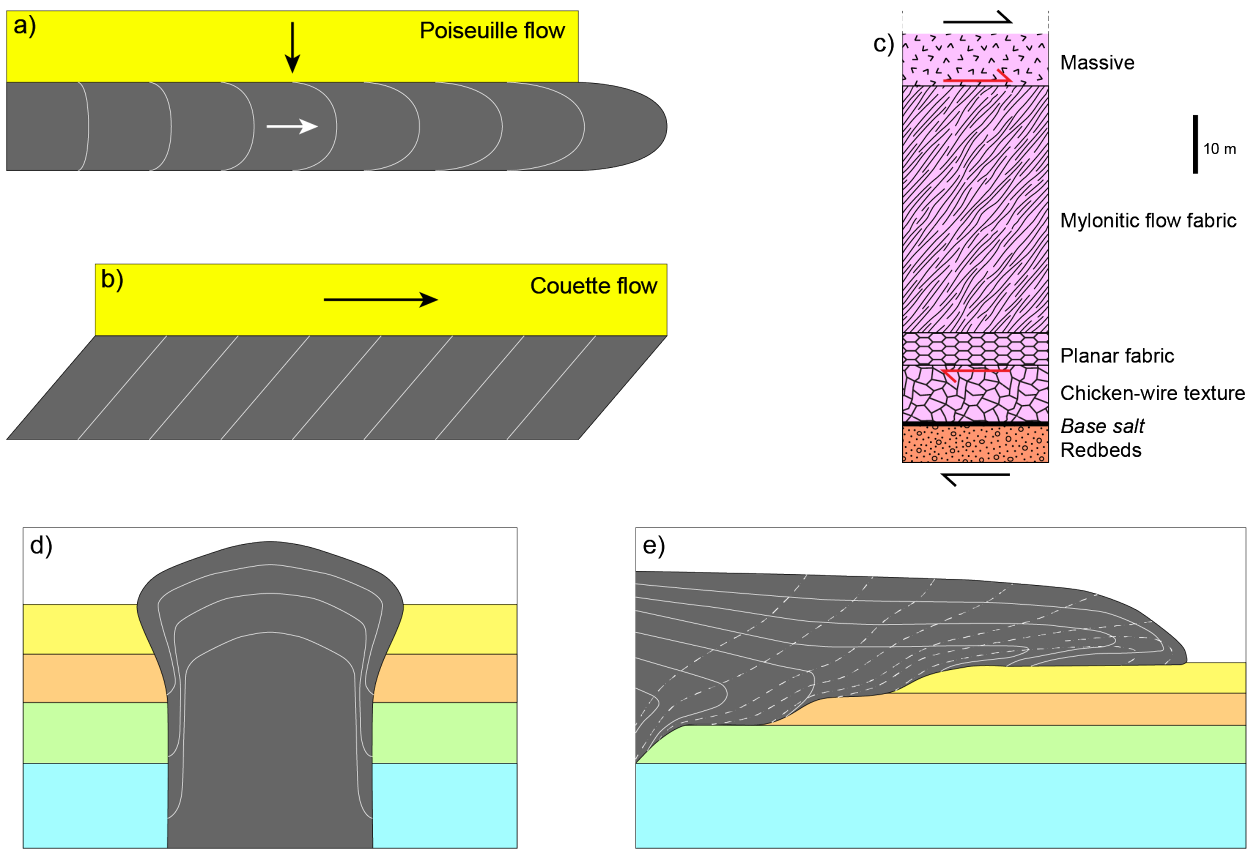

Figure 2*. Viscous (boundary) drag at the edges of a salt layer (or a diapir if rotated 90º): a) and b) theoretical internal flow in Poiseuille and Couette flow, respectively (white lines are imaginary, originally vertical lines) (modified from Rowan, 2020); c) field observations of the basal portion of a salt detachment (lavender indicates gypsum) in the Sierra Madre Oriental of Mexico (black arrows show overall translation, red arrows show zone of concentrated shear; modified from Cross, 2012); d) and e) salt stock/wall and salt sheet, respectively, with internal viscous flow that is concentrated near the edges indicated by white lines (solid – originally horizontal; dashed – originally vertical; no scale; modified from Jackson and Hudec, 2006).*

3.1. Models

3.1.1. Salt stocks/walls

Most early models, beginning with Nettleton (1934), assumed that both the salt and the overburden behaved as viscous materials such that diapirism was driven by density contrasts and Raleigh-Taylor overturn (e.g., Nettleton, 1943; Dixon, 1975; Ramberg, 1981; Jackson and Cornelius, 1987; Schmeling et al., 1988; Podlachikov et al., 1993). In these cases, of course, deformation of material surrounding the salt was by viscous flow. Yet it was Nettleton himself (Nettleton and Elkins, 1947; Nettleton, 1955) who subsequently questioned this approach due to the inability of viscous models to reproduce the faulting commonly present around Gulf Coast salt domes (e.g., Wallace, 1944) and thus began using granular materials to simulate the overburden. Other early models also used weak salt analogs but stronger surrounding material (e.g., Parker and McDowell, 1951, 1955; Withjack and Scheiner, 1982; Lemon, 1985), and almost all experimental and numerical modeling of diapirs during the past three decades has followed this approach (e.g., Vendeville and Jackson, 1992; Davison et al., 1993; Schultz-Ela et al., 1993; Daudré and Cloetingh, 1994; Vendeville and Nilsen, 1995; Alsop et al., 1995; Alsop, 1996; Fredrich et al., 2003; Schultz-Ela, 2003; Dooley et al., 2005; Yin and Groshong, 2007; Yin et al., 2009; Sanz and Dasari, 2010; Nikolinakou et al., 2012, 2014, 2017; Callot et al., 2016; Karam and Mitra, 2016; Heidari et al., 2017, 2019; Ferrer et al., 2018).

Many of the models generated folds of strata flanking and above the diapirs. Parker and McDowell (1955) attributed the folding to arching and penetration of the roof by the salt, with possibly some component of frictional drag. Similarly, Schultz-Ela (2003) demonstrated that folding is due to rotation of roof flaps during drape folding (Fig. 3a), with drag folds developing only if the surrounding material has strength comparable to that of the salt. In contrast, other models attributed folding to drag/shear of the flanking strata (e.g., Lemon, 1985; Alsop et al., 1995).

A related element of many experimental and numerical model results was bed thinning and lengthening during folding above and adjacent to diapirs (e.g., Lemon, 1985; Davison et al., 1993; Alsop et al., 1995; Alsop, 1996; Schultz-Ela, 2003; Nikolinakou et al., 2018a). This was also the case for experimental-model halokinetic megaflaps (Callot et al., 2016), which are minibasin-scale zones of upturned and thinned strata (Rowan et al., 2016). Interestingly, numerical-model megaflaps experience initial bed lengthening and then bed shortening (Nikolinakou et al., 2017). Both sets of models used relatively weak materials or material properties; in contrast, an experimental model with a mixture of clay and sand to give more cohesion and strength to the overburden resulted in minimal thinning and lengthening of megaflaps (Ferrer et al., 2018).

A common type of near-diapir structure produced in early experimental models of salt stocks, which tended to use clay or similar materials, are faults in the roofs over the crests of diapirs. In the absence of applied regional stress, these comprise primarily extensional radial faults, commonly with central ring-like patterns with downdropped centers (Fig. 3b), due to doming of the roof and consequent hoop stress (e.g., Parker and McDowell, 1955; Withjack and Scheiner, 1982; Alsop, 1996; Yin and Groshong, 2007; Yin et al., 2009). Fault arrays observed in models are more linear in the case of salt walls, with both crestal grabens bounded by inwardly-dipping normal faults and crestal highs bounded by inwardly-dipping reverse faults (e.g., Davison et al., 1993; Schultz-Ela et al., 1993). Furthermore, modeled diapir dissolution generated steep supra-diapir faults, some of which rotated into reverse-fault orientations due to associated folding (Ge and Jackson, 1998).

Numerical or analytical models of diapirs have not generally produced discrete faults or fault zones (exceptions include, e.g., Schultz-Ela et al., 1993). However, near-diapir stress can be quantified and used to infer likely structures such as fractures. Because of salt's inability to maintain deviatoric stress and the consequent isotropic intrasalt stress regime, principal stresses

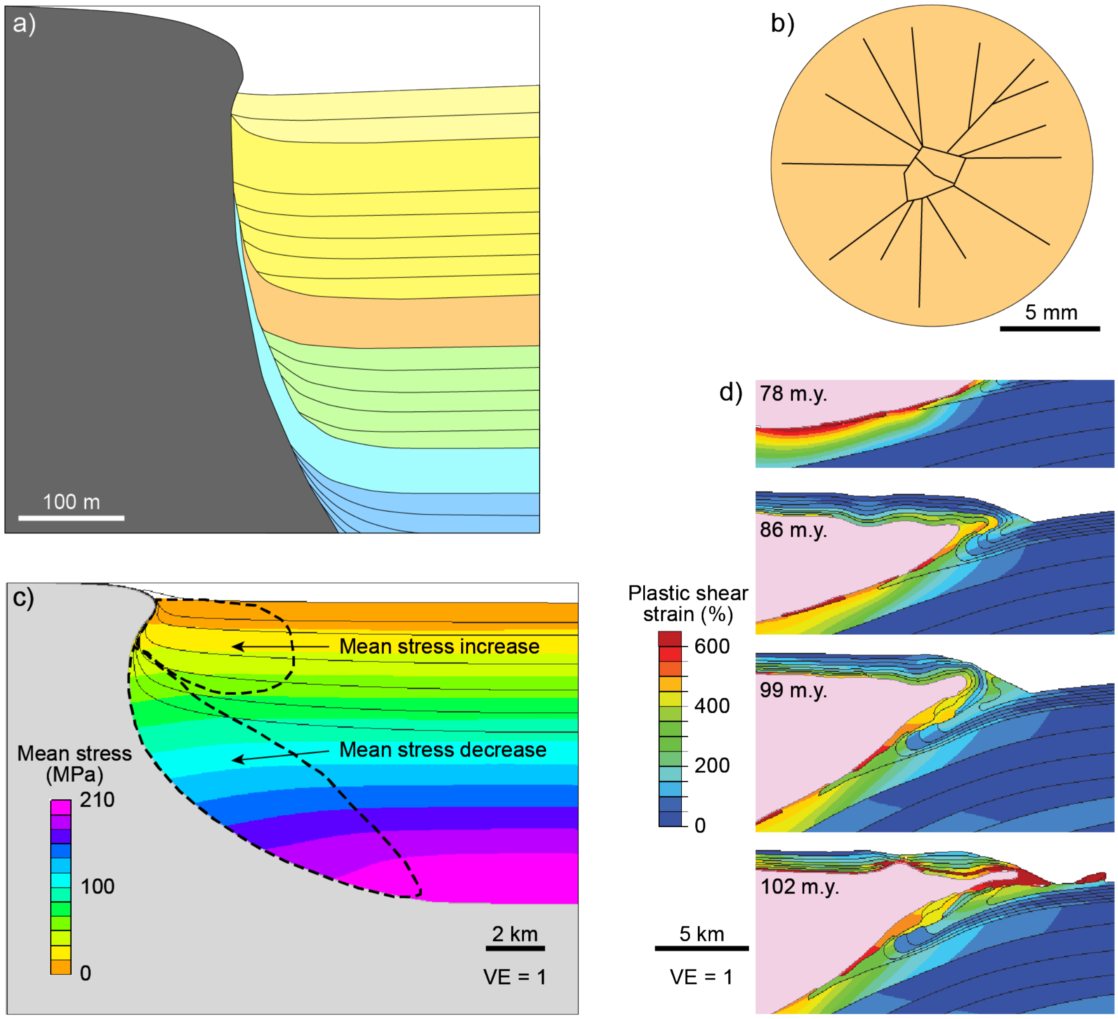

***Figure 3**. Modeled near-diapir deformation: a) numerical model of syndepositional drape (flap) folding adjacent to salt wall (in grey; modified from Schultz-Ela, 2003); b) experimental model of radial and concentric faults in domed strata above salt stock (modified from Alsop, 1996); c) numerical model showing mean stress adjacent to salt diapir (in grey) after 5 m.y. (modified from Nikolinakou et al., 2014); d) numerical model showing evolving plastic shear strain in thinned, stretched, overturned roof layers beneath salt sheet (in pink; modified from Nikolinakou et al., 2019). VE is vertical exaggeration.*

in flanking strata are reoriented and vary in magnitude compared to far-field stress patterns (e.g., Fredrich et al., 2003; Koupriantchik et al., 2005; Sanz and Dasari, 2010; Luo et al., 2012; Nikolinakou et al., 2012). The increase in horizontal stress and decrease in concentric (hoop) stress in the upper parts of diapirs (Fig. 3c) has been invoked to cause radial faulting due to lateral expansion of the diapir, so-called stem push (e.g., Luo et al., 2012; Nikolinakou et al., 2014, 2017, 2018a; Heidari et al., 2017). Similarly, elevated in situ shear stress resulting from increased pore pressure adjacent to a diapir just above a dipping permeable bed may be great enough to cause shearing of diapir-flanking strata (Heidari et al., 2019). In another approach, analytical modeling suggests that during contractional narrowing of a diapir, the wall rocks remain undeformed until a critical width is attained (effectively an incomplete weld, with <50 m of remnant salt), at which point strain is transferred to the wall rocks (Davies et al., 2010).

3.1.2. Salt sheets

Salt glaciers have been generated in numerous analog models, especially during squeezing of salt stocks/walls or by extrusion from the basinward edge of salt, but were usually not the focus of those experiments (e.g., Koyi et al., 1993; Koyi, 1996; Gemmer et al., 2005; Rowan and Vendeville, 2006; Ings and Shimeld, 2006; Callot et al., 2007, 2012; Albertz et al., 2010; Albertz and Ings, 2012; Adam and Krezsek, 2012; Warsitzka et al., 2013; Wu et al., 2015; Gradmann and Beaumont, 2016; Duffy et al., 2018). Other experiments specifically addressed salt sheets but examined aspects such as suturing between separate sheets or the dismembering and rafting of sheet roof/carapace during spreading of the salt (Dooley et al., 2012; 2014). There have been very few attempts to model salt sheet emplacement and advance. Early numerical models invoked sill-like intrusion into sediment (Cao et al., 1989; Yu et al., 1991), but we now accept that most salt sheets are emplaced either at the surface as salt glaciers or just beneath the surface, with the salt and its roof advancing on short thrust faults that emerge at the sea floor (Hudec and Jackson, 2006, 2009; Hearon et al., 2015a; Rowan, 2017).

Numerical models show that stresses can deviate from regional values above, below, and at the tips of salt sheets. Specifically, vertical stress is slightly elevated next to the edges and horizontal stress is significantly reduced both above and below (Fredrich et al., 2003). The reduction in shear strength and possible consequent shear failure may explain so-called rubble zones (intervals of disrupted and mixed strata) beneath some sheets (Fredrich et al., 2003, 2007). Modeling also suggests that pore pressure is increased below salt, elevating deviatoric stress and further enhancing the likelihood of subsalt shear failure, especially toward the front of the sheet (Nikolinakou et al., 2018a, 2018b). Plastic shear strain in stretched, thinned, and overturned model sediments beneath sheets can be as high as 600% (Fig. 3d; Nikolinakou et al., 2019). Even ignoring the effects of pore pressure, modeling of advancing sheets predicts that the maximum shear stress is at the base of the sheet and that there is strong horizontal contraction in sediments in front of the toe (Li and Fischer, 2017).

Welding of a salt layer, whether allochthonous or autochthonous, might lead to further effects on adjacent sediments. Modeling shows that stresses are concentrated near weld tips, with abrupt lateral gradients (Heidari et al., 2016). Thus, as welding propagates along the salt layer, a near-vertical zone of high shear deformation in overlying strata might move laterally, progressively generating steep suprasalt faults.

3.2. Empirical data

Numerous investigations of observed near-diapir deformation have been reported. These include both subsurface analyses, based on seismic and well data, and outcrop studies of exposed salt stocks/walls and sheets. In the sections below, we review observations and interpretations of folds, faults, other fractures, and shear zones, first adjacent to steep diapirs, then beneath salt sheets, and finally next to salt welds. Note that we will return to some of the examples later when we offer our current thoughts and understanding.

3.2.1. Salt stocks/walls

3.2.1.1. Folds

Near-diapir folding has been recognized from the onset of studies of diapirs (e.g., Pošepný, 1871; Choffat, 1882; Veatch, 1899; see Jackson, 1995). Folds may be related either to regional tectonics (e.g., contractional anticlines or extensional rollovers that intersect the diapirs) or to diapir rise itself. We focus solely on the latter, in which stratal upturn and thinning have generally been attributed to two very different processes. First, the upturn has been considered to be a result of drag or shear of flanking strata by the rising salt (e.g., Murray, 1966, 1968; Bornhauser, 1969; Lemon, 1985; Jackson et al., 1990; Alsop et al., 1995, 2000; Roca et al., 1996; Davison et al., 2000a; Stewart, 2006). In such drag models, observed stratal thinning has been explained as primarily structural rather than depositional (Fig. 1c).

Others have noted that thinning is primarily depositional (e.g., Parker and McDowell, 1955; Brinkmann and Lötgers, 1968; Johnson and Bredeson, 1971; Worrall and Snelson, 1989). Thus, the second model for upturn and thinning of near-diapir strata invokes near-surface drape folding of the diapir roof as sediment is deposited over or onlapping the diapiric topographic high. Fluctuations in the local ratio between salt-rise rate and sediment-accumulation rate generate stacked, unconformity-bound stratal packages termed halokinetic sequences and composite halokinetic sequences (Fig. 4a), originally identified in La Popa Basin, Mexico (Giles and Lawton, 2002; Rowan et al., 2003; Giles and Rowan, 2012; also termed perched flaps by Jackson and Hudec, 2017). Halokinetic sequences have since been interpreted in both outcrop and the subsurface globally (e.g., Lawton and Buck, 2006; Andrie et al., 2012; Kernen et al., 2012; Carruthers et al., 2013; Ringenbach et al., 2013; Callot et al., 2014; Hearon et al., 2014, 2015a, 2015b; Harrison and Jackson, 2014; Lopez-Mír et al., 2014, 2017; Saura et al., 2014, 2016; Poprawski et al., 2014, 2016; Lawton et al., 2015; Rojo et al., 2016; Martín-Martín et al., 2016; Kergaravat et al., 2016, 2017; Rojo and Escalona, 2018; Coleman et al., 2018; Asl et al., 2019; Pichat et al., 2019; Snidero et al., 2019; Davison and Barreto, 2019; Mount et al., 2019; Pichel and Jackson, 2020; Gannaway-Dalton et al., 2020a). In a somewhat different interpretation that combines elements of both drape and drag folding, drape folds were interpreted to have formed not by flexural slip, as shown by Rowan et al. (2003), but by diapir-parallel shear of relatively unconsolidated sediment (Alsop et al., 2016).

Similarly, halokinetic megaflaps (Fig. 4b), which are characterized by upturned and thinned deep minibasins strata, are a larger-scale form of syndepositional drape folding between a rising salt body and a sinking minibasin (Rowan et al., 2016). They have been increasingly recognized in several salt basins (e.g., Giles and Rowan, 2012; Graham et al., 2012; Rowan et al., 2016; Martín-Martín et al., 2017; Escosa et al., 2018; Thompson Jobe et al., 2019; Gannaway-Dalton et

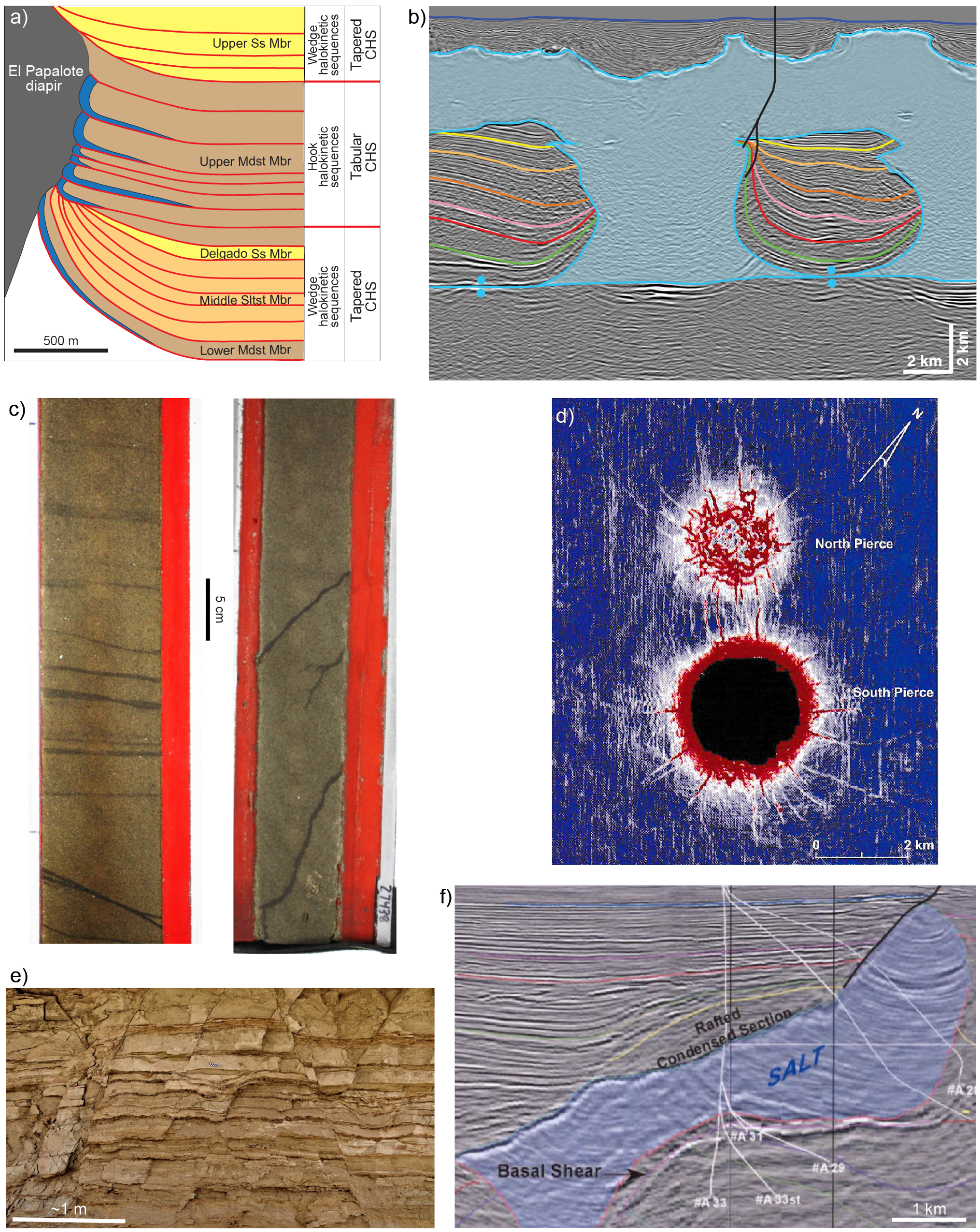

Figure 4. *Outcrop and subsurface observations: a) summary of drape-fold halokinetic sequences and composite halokinetic sequences (CHS) adjacent to El Papalote diapir, La Popa Basin (Ss – sandstone; Sltst – siltstone; Mdst – mudstone; blue – carbonate lentils) (modified from Giles and Rowan, 2012); b) halokinetic megaflap proven by wells (black lines) in the northern Gulf of Mexico (modified from Rowan et al., 2016); c) core photographs showing deformation bands in sandstones near a salt wall in the northern Gulf of Mexico (modified from Wilkins et al., 2019); d) dip map from seismic data in the Central North Sea showing radial faults next to South Pierce diapir and radial and concentric faults above North Pierce diapir (Jackson and Hudec, 2017); e) photograph of exposed strata near Mt. Sedom diapir with conjugate sets of small extensional faults (Alsop et al., 2018); f) interpreted seismic profile from the northern Gulf of Mexico with subsalt rubble zone identified as basal shear zone (Harrison et al., 2004).*

al., 2020b), and other examples can be found in the older literature (e.g., Schachl, 1987; Baldschuhn, 2001; Stovba and Stephenson, 2002).

The folds described so far involve strata dipping away from the salt, but there are also cases where the strata fold down toward the salt. These comprise both minibasin-scale features such as turtle structures or expulsion-rollover structures, which record differential subsidence into a salt layer (e.g., Trusheim, 1960; Ge et al., 1997), and smaller-scale folds formed over the edge of the top salt or over local salt shoulders. The latter have been identified in several salt basins (e.g., Eskozha, 2008; Hearon et al., 2015a; McFarland, 2016; Giles et al., 2018; Escosa et al., 2018; Gannaway-Dalton et al., 2020b; Langford et al., 2020).

3.2.1.2. Faults

Near-diapir faulting was recognized early on to be common above and around many salt walls and stocks (e.g., Wallace, 1944; Behrmann, 1949; Parker and McDowell, 1951; Murray, 1966, 1968; Hempel, 1967; Brinkmann and Lötgers, 1968; Contreras and Castillón, 1968; Dalgarno and Johnson, 1968; Johnson and Bredeson, 1971). Again, we focus here on faults related to diapir rise itself rather than regional extensional, contractional, strike-slip, or salt-evacuation faults, which have specific trends and often curve to intersect the diapirs. Also, we discuss here larger faults that would be apparent on high-quality seismic data (tens of m of displacement or more), addressing smaller fractures in the next section.

Radial extensional faults have been observed both over the crests of buried diapirs and around diapir flanks (Fig. 4d) (e.g., Hempel, 1967; Brinkmann and Lötgers, 1968; Davison et al., 2000a; Rowan et al., 2003; Stewart, 2006; Quintà et al., 2012; Carruthers et al., 2013; Salazar et al., 2014; Harding and Huuse, 2015; Coleman et al., 2018; Mattos and Alves, 2018; Maunde and Alves, 2020). Those above the diapirs have been attributed to doming and the consequent concentric tensile stress. Those on the flanks, though, have been interpreted in two different ways. First, they may have formed in roof strata and been rotated into diapir-flanking positions by drape folding and the development of halokinetic sequences (Rowan et al., 2003). Alternatively, they may have formed in place by stem push facilitated by hoop stress (Jackson and Hudec, 2017; Coleman et al., 2018). Radial faults are common on stocks but are concentrated at the ends of salt walls (e.g., Davison et al., 2000a; Stewart, 2006; Lawton et al., 2015; Escosa et al., 2018). Radial thrusts have also been interpreted and were attributed to collapse of a diapir stem and consequent inward movement of surrounding strata (Jackson et al., 1998).

Diapir-parallel faults have three reported origins. First, they may be crestal normal faults caused by doming of the roof, in which case they are somewhat polygonal in map view and termed concentric faults above salt stocks (Fig. 4d) but are linear above salt walls (e.g., Brinkmann and Lötgers, 1968; Davison et al., 2000a; Stewart, 2006; Yin and Groshong, 2007). Second, some faults have been suggested to form in flanking positions as either extensional faults caused by collapse of the diapir stem or thrust faults generated by stem push (Jackson et al., 1998; Stewart, 2006; Jackson and Hudec, 2017). Third, halite dissolution and collapse of the roof into the salt typically produces steep diapir-parallel faults (e.g., Eskozha, 2008; Krzywiec, 2009; McFarland, 2016; Escosa et al., 2018; Thompson Jobe et al., 2019).

3.2.1.3. Small-scale deformation

Diapir rise has been associated in the literature with not just folding and seismic-scale faulting, but also small-scale deformation such as small-offset faults, other fractures, and shear/gouge zones. Because these features are below the resolution limits of seismic data, observations and interpretations are from outcrop examples and wells. Below, we review first well data and then outcrop observations.

Well analyses have been somewhat contradictory due to differing opinions on how diapirs form. Hanna (1953) noted primarily radial fractures in competent beds and fractured, brecciated textures in incompetent shales close to the diapirs. Kerr and Kopp (1958) interpreted so-called salt-dome breccias in shales that extended roughly 1 km laterally and above diapirs, and invoked compaction and brecciation of 'invaded' shales by the salt. Early reports also commonly noted gouge zones within diapir-flanking 'shale sheath' (see Fig. 1a), which supposedly formed by drag/shear of pre-diapiric shales during salt intrusion (e.g., Kerr and Kopp, 1958; Murray, 1966, 1968). In contrast, others rejected this interpretation and interpreted shale sheath as the roof of early salt structures that subsided as new sediments were deposited (Johnson and Bredeson, 1971; Worrall and Snelson, 1989).

Davison et al. (2000b) noted extensional fractures and brecciated fault zones in wells above and around Central North Sea diapirs. The fractures formed conjugate sets about bedding, with the abundance and intensity greatest close to the diapir and decreasing to zero 800 m from the diapir. The fracture patterns, combined with observations of soft-sediment, fluidized breccias, were interpreted by Davison et al. (2000b) as very early extensional thinning and gravitational failure of the roof as the diapirs penetrated their overburden. More recently, Wilkins et al. (2019) evaluated deformation bands and small-offset faults from well cores along a salt wall in the northern Gulf of Mexico (Fig. 4c). Diapir-parallel deformation bands were attributed to flexural-slip folding during diapir growth, and radial deformation bands were related to along-strike variations in the geometry of the salt-sediment interface, with the greatest concentration at a prominent bend in the salt wall.

Published outcrop analyses of small-scale deformation adjacent to stocks and walls also differ significantly in their observations and interpretations. In an influential paper, Alsop et al. (2000) noted several features near diapirs in Nova Scotia: minor extensional faults forming conjugate sets within bedding that thus formed early; later, diapir-parallel minor faults recording relative uplift of the salt (Fig. 1d); and pervasive granulation seams on one flank of one diapir. They attributed the deformation to attenuation and shear of overburden in drag zones adjacent to the diapirs. Similarly, the Mt. Sedom diapir in Israel has early conjugate and domino sets of small extensional faults (Fig. 4e) and diapir-parallel extensional faults with diapir-side up, also interpreted as recording passive (shear) folding, albeit with an overprint of strike-slip deformation (Alsop et al., 2016, 2018). In the Sivas Basin of Turkey, two localities have cm to 1 m thick shear zones adjacent to the salt with clasts of gypsum/anhydrite embedded in fractured shale gouge (Collon et al., 2016).

In contrast, others have noted little small-scale deformation adjacent to stocks and walls, and specifically none that records diapir-parallel shear or drag. In La Popa Basin, ignoring regional fractures and cleavage related to orogenic shortening, halokinetic drape-folded sediments have two relatively minor fracture sets: those radial to the diapirs, and those recording outer-arc extension of tightly folded strata (Rowan et al., 2003). In the Basque Pyrenees, and again ignoring regional deformation, brittle deformation is insignificant at Bakio diapir (Poprawski et al., 2014). In the same basin, analyses of fractures at Poza de la Sal diapir showed two different patterns: 1) in the oldest conformable suprasalt strata that are now near-vertical next to the salt, three sets of bedding-perpendicular fractures record early salt movement (Hempel, 1967); and 2) joints in younger, domed strata farther from the diapir are radial, similar to the larger faults (Quintà et al., 2012). Investigation of outcrops in the La Popa, Lusitanian, and Nova Scotia salt basins suggested that differential stress was insufficient to cause sediment failure but large enough for minor, distributive grain fracturing (Davies et al., 2010). Small-scale deformation is also minor to nonexistent in exposed megaflaps (e.g., Graham et al., 2012; Rowan et al., 2016; Canova, 2017). Interestingly, the only diapir-parallel shear noted has a diapir-down sense, the opposite of that expected for drag induced by diapir rise, and probably developed due to flexural-slip folding on the megaflap limb (Canova, 2017).

3.2.2. Salt sheets

Fewer published analyses exist that address observed deformation associated with salt-sheet emplacement and advance. Large-scale folds are rare beneath sheets compared to adjacent to stocks/walls. Base-salt flats generally have no folding, whereas ramps may have halokinetic folds of overturned roof strata (Kernen et al., 2012; Callot et al., 2014; Hearon et al., 2015a; Rowan, 2017) and the transition from steep diapir to subhorizontal salt may also have bedding folded from vertical to overturned (Davison et al., 1995, 1996). Similarly, seismic-scale faults are relatively uncommon. Thrust faults and imbricates that formed during salt emplacement were interpreted beneath salt sheets in the northern Gulf of Mexico (Harrison and Patton, 1995; Jackson and Hudec, 2004; Hudec and Jackson, 2006, 2009), but exposed analogs in South Australia show only a single minor subsalt thrust beneath one sheet (Kernen et al., 2012; Hearon et al., 2015a, 2015b; Rowan et al., 2019a). Fiduk et al. (2016) noted extensional and thrust faults detached on overpressured shales beneath salt canopies in the northern Gulf of Mexico (Fig. 5) and attributed them to post-emplacement sediment failure due to loading by the overlying salt.

Likewise, there are conflicting reports on the presence and nature of small-scale deformation beneath salt sheets. Numerous wells in the northern Gulf of Mexico have encountered intervals immediately beneath the salt termed rubble zones (also known as gumbo zones) that are structurally disrupted and usually yield mixed biostratigraphic ages. These have been interpreted variously as subsalt shear zones (Figs. 1a, 4f) (e.g., Harrison and Patton, 1995; Harrison et al., 2004; Willson and Fredrich, 2005), areas of in situ failure due to high pore pressures (e.g., House

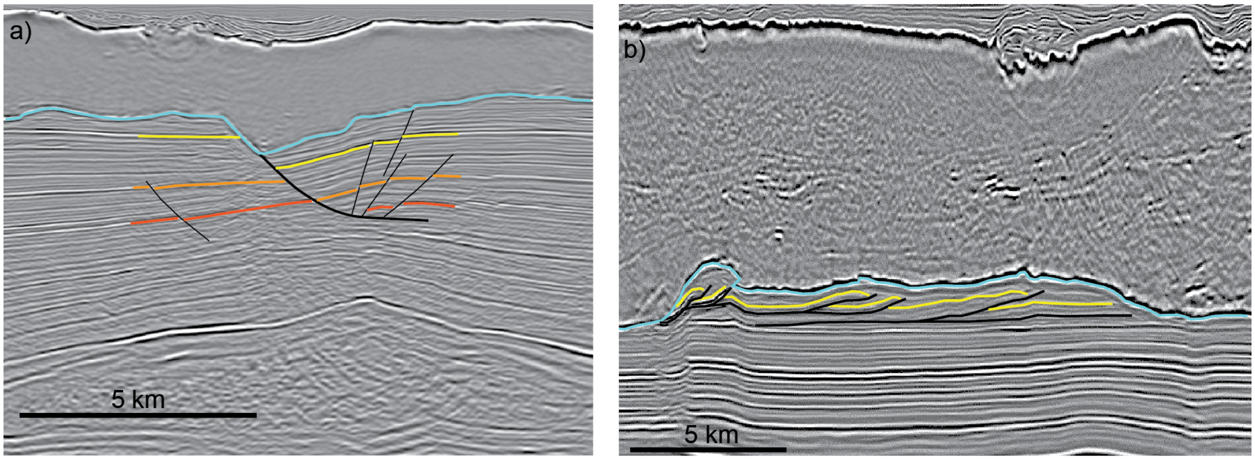

Figure 5. *Subsalt faulting in the northern Gulf of Mexico (modified from Fiduk et al., 2016): a) extensional fault detached in overpressured shales and offsetting base of salt sheet to form a prominent keel (no vertical exaggeration); b) thrust imbricates folding and offsetting base of salt sheet (2:1 vertical exaggeration). Base salt in blue, faults in black, unspecified horizons in other colors.*

and Pritchett, 1995; Willson and Fredrich, 2005), or areas of slumped carapace that was overridden by the advancing salt (e.g., Kilby et al., 2008; Hearon et al., 2015a; Rowan, 2017). Field observations in South Australia have also been interpreted differently: whereas Hearon et al. (2015a) found no evidence of subsalt shear zones or rubble zones, Williams et al. (2019) interpreted subsalt asymmetric folds as probably forming during salt emplacement due to soft-sediment deformation or subsalt shear. Similarly, Davison et al. (1995, 1996) interpreted asymmetric small-scale folds to be caused by shear beneath a horizontal salt glacier. In the gypsiferous Sivas Basin, base-salt flats have no shear-related structures beneath the salt-sediment interface but two ramps have shear zones just beneath the sheets up to 1 m thick with sandstone and gypsum lenses and boudins, gouge and breccia, small faults, and rotated blocks (Kergaravat, 2016; Kergaravat et al., 2017).

3.2.3. Salt welds

Outcrop studies of salt welds are rare. Rowan et al. (2012) showed that the amount of small-scale deformation varied along the length of a 24 km long vertical (secondary) weld in La Popa Basin: where it is not actually welded, with >50 m of remnant gypsum, strain is negligible; where it is a discontinuous weld, wall rocks show increased fracturing within 15 m of the weld; and where it is completely welded, with post-welding weld-parallel slip, a damage zone several 10s of m in thickness developed, with sheared and highly fractured siliciclastic rocks juxtaposed against slightly fractured carbonates. Similarly, Smith et al. (2012) showed that most veins along the same weld formed after weld formation and are most abundant on the inside of a prominent bend in the weld trace.

An allochthonous (tertiary) weld in South Australia has somewhat enigmatic patterns of veins, joints/tension gashes, and small faults (Williams et al., 2019). Above the sheet, veins are concentrated above remnant salt rather than the laterally equivalent weld (in contrast to the models of Heidari et al., 2016) and decrease in abundance away from the salt, whereas there is no clear pattern beneath the salt. Williams et al. (2019) concluded that the small-scale deformation most likely occurred either during evacuation and welding or after welding (during orogenic shortening). Similarly, it is unclear whether damage zones along allochthonous welds in the Sivas Basin (Jackson and Hudec, 2017, fig. 9.5a) formed due to welding or regional shortening (see, e.g., Kergaravat et al., 2016).

4. Near-diapir deformation

The summary of the existing literature above reveals significant differences in models, observations, and interpretations of near-diapir deformation. Below, we offer our collective assessment of this topic, but utilizing mostly relationships around exposed diapirs due to the assumptions and limitations inherent in models and subsurface data. Our personal experience, gained through intensive fieldwork or short visits, includes the Paradox Basin of the southwest USA, La Popa Basin in northeastern Mexico, Nova Scotia, the Spanish Pyrenees, the Prebetics of SE Spain, the Northern Calcareous Alps of Austria, Mt. Sedom diapir in Israel, the Sivas Basin of Turkey, the Fars province of the Zagros Mts., the Kuqa fold-and-thrust belt of NW China, and the Flinders and Willouran Ranges of South Australia. We will address in order folds, seismic-scale faults, and small-scale deformation around both salt stocks/walls and salt sheets.

4.1. Folds

4.1.1. Folds associated with regional tectonics

Salt basins have all manner of folds caused by various processes. At one end of the spectrum are larger-scale structures with both lengths and wavelengths of multiple kilometers, with one subset of these comprising those generated by regional tectonic or gravity-driven deformation. Folds associated with extension tend to be confined to one flank of stocks and walls. For example, extensional hanging-wall rollovers are characterized by strata that are folded down toward the diapirs (e.g., López-Mir et al., 2014), formed as one flanking minibasin moves laterally relative to that on the other side of the diapir during thin-skinned extension.

More prominent, though, are contractional salt-cored anticlines or thrusted anticlines. If shortening occurs after passive diapirs are already established, the weak diapirs usually localize the contractional strain such that they get squeezed, with contractional folds often extending away from the stocks or walls in linear or polygonal patterns depending on the original diapir/minibasin configuration (e.g., Letouzey and Sherkati, 2004; Rowan and Vendeville, 2006; Callot et al., 2007, 2012; Jahani et al., 2009; Saura et al., 2014). Salt sheets may emanate from squeezed feeder diapirs in the cores of anticlines or may be modified by underlying folds (e.g., Hudec et al., 2009; Rowan et al., 2019a).

4.1.2. Minibasin-scale folds

The other subset of larger-scale folds comprises those related to loading-induced salt evacuation and inflation. These may be simple synclinal folds or monoclinal halokinetic megaflaps (Fig. 6), with strata gradually steepening toward the diapirs. In both cases, growth strata may be characterized by simple thinning and wedging, prominent onlap, or, more rarely, erosional unconformities (e.g., Gannaway et al., 2020b). In turtle structures and expulsion-rollover structures, which are minibasin-scale folds caused by bidirectional or unidirectional progressive salt evacuation, respectively, strata tend to dip toward the diapir over distances of multiple kilometers. Some of the best outcrops of minibasin-scale folds are found in the cross-sectional exposures of the eastern Willouran Ranges of South Australia (e.g., Hearon et al., 2015b).

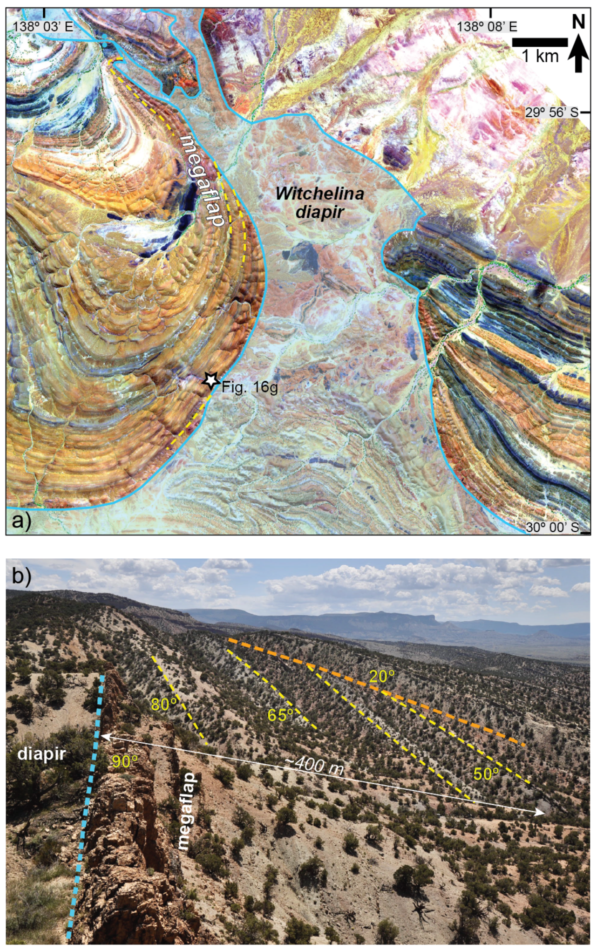

Figure 6. *Exposed halokinetic megaflaps: a) Witchelina diapir (Willouran Ranges, South Australia) with megaflap and growth strata in minibasin-scale drape fold (modified from Rowan et al., 2016; see also Gannaway Dalton et al., 2020b); b) megaflap and growth strata adjacent to Gypsum Valley diapir, Paradox Basin, Colorado (location shown in Fig. 15c; see Escosa et al., 2018). Blue lines are edge of salt, yellow lines show bedding, orange line is an unconformity, and numbers indicate average stratal dip.*

4.1.3. Local halokinetic folds

Most steep diapirs are also characterized by local folds, where minibasin strata turn up abruptly within distances from 10 m to 1.3 km from the salt, with most folds 100-800 m wide (Fig. 7). As already mentioned, these have been the source of considerable differences in interpretation, with folding and thinning attributed to either drag/shear of adjacent strata or syndepositional drape folding accompanying passive rise.

We have yet to see an exposed example of originally constant-thickness strata that were thinned and sheared due to upward salt rise or lateral salt emplacement. Instead, abundant evidence from a variety of tectonic and depositional settings demonstrates variable and fluctuating topographic relief over growing diapirs, with strata thinning depositionally onto the highs. First, stacked sequences of upturned and thinned strata are separated by local angular unconformities that usually terminate against the salt at cusps in the salt-sediment interface and that become conformable within a short distance of the salt edge (Fig. 7). Second, local depositional breccias extend out into, and usually thin away from, the diapirs, commonly just above the unconformities (Figs. 7a, b, e, 8a). These reworked sediments sometimes contain clasts derived from the diapirs themselves (e.g., Giles and Lawton, 2002). Third, local facies changes indicate shallower water depths over and close to the diapirs compared to within the minibasins (Figs. 8b, c), as observed in both carbonate and siliciclastic facies in La Popa Basin (e.g., Aschoff and Giles, 2005; Giles et al., 2008).

The observed features are characteristic of halokinetic sequences and composite halokinetic sequences (Giles and Lawton, 2002; Rowan et al., 2003; Giles and Rowan, 2012). In the case of a salt stock/wall, drape folding of syndepositional strata over the shallow diapir breaks the roof (Fig. 9a) and rotates roof flaps into diapir-flanking positions as new roof is deposited; thus the edge of salt in any position represents a paleo top salt that was rotated along with its roof (Fig. 9b). If the roof strata are concordant with the top salt, they end up with approximately the same dip as the edge of the diapir (Figs. 7a, 9c top); if the strata onlap the top salt, they end up less steep or overturned than the edge of salt (Figs. 7d, 9c bottom).

A key observation in distinguishing between drag/shear versus synsedimentary drape folding around diapirs is the presence of stacked unconformities separating discrete packages of upturned and thinned strata. Moreover, in none of the field examples we have examined (e.g., La Popa, Pyrenees, Zagros, Sivas; Fig. 7) are the unconformities cut or affected by diapir-parallel faults or shears.

Depending on the mechanical properties of the multilayer, folding is accommodated by some combination of flexural flow, flexural slip, and orthogonal flexure. There are usually enough interbedded weak shales or marls so that the primary deformation mechanism during drape folding is flexural slip/flow, i.e., slip or shear parallel to bedding (Rowan et al., 2003, 2016; Rowan and Ratliff, 2012). If the strata were deposited with convergent geometries, thinning over the diapir, flexural shear within the weak layers narrows the overall taper angle of the stratal wedge during folding, thereby appearing to stretch and thin the beds (Fig. 9d, left; Hearon et al., 2014). The same process decreases stratal truncation angles against salt and increases the

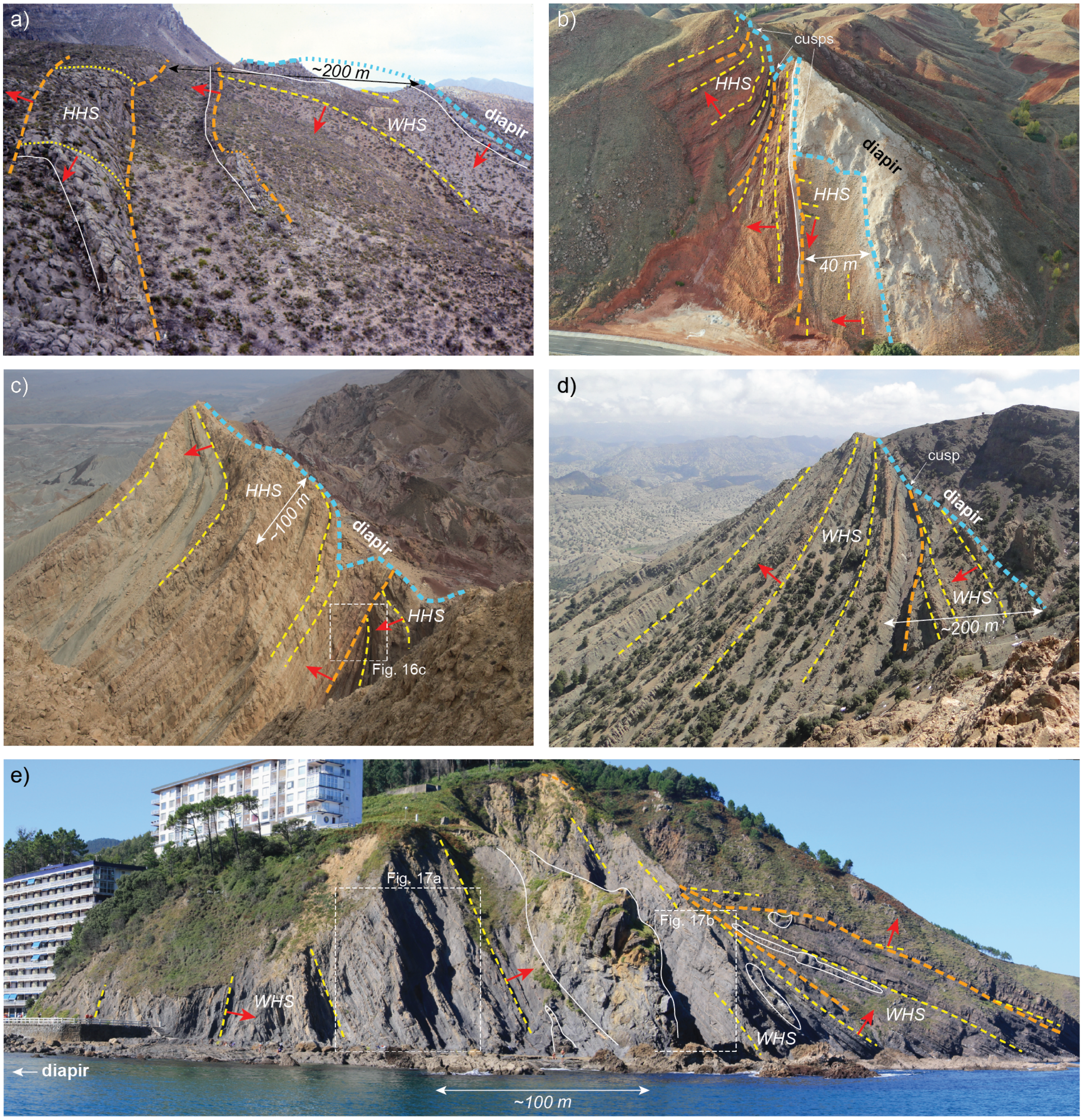

***Figure** 7. Diapir-flanking drape folds: a) hook and wedge halokinetic sequences (HHS and WHS, respectively) in shallow-water mixed siliciclastics and carbonates at El Papalote diapir, La Popa Basin (location shown in Fig. 15a); b) margin of Ilkindi minibasin, Sivas Basin, with two HHS in nonmarine redbeds separated by a cusp at the edge of salt (drone photography by J.-C. Ringenbach); c) stacked HHS in shallow-water limestones at Ilcheh diapir, Fars province, Zagros Mts.; d) stacked WHS in marls at Tassent diapir, High Atlas Mts. (photo courtesy of R. Joussiaume); e) stacked WHS in deepwater marls and turbidites at Bakio diapir, Basque Pyrenees. Yellow lines trace bedding; orange lines mark local unconformities; red arrows show stratigraphic up; white lines outline or indicate the top of depositional breccias.*

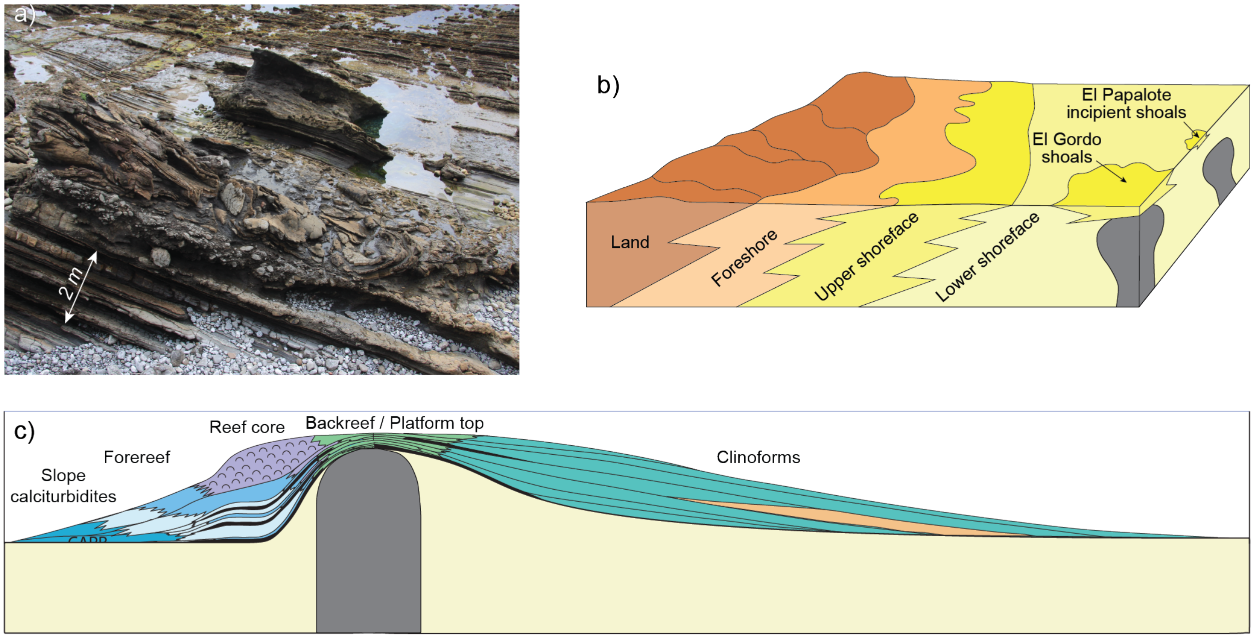

Figure 8. *Sedimentologic evidence for syndiapiric topographic relief: a) locally derived mass-transport deposit within deepwater turbidites adjacent to Bakio diapir, Basque Pyrenees; b) cartoon showing local shoaling over diapirs (grey) in La Popa Basin (modified from Aschoff and Giles, 2005); c) schematic diagram of carbonate facies distribution at El Gordo diapir, La Popa Basin, controlled by both seafloor topography and wind direction (modified from Giles et al., 2008).*

distance between individual cutoffs during folding (Fig. 9d, left). If the strata are dominated instead by thick, competent beds, they may deform by orthogonal flexure with a component of flexural slip on widely spaced weak layers (Fig. 9d, right). This results in minor cusps at the salt-sediment interface and little change to cutoff angles and distances (Fig. 9d, right). A similar process of convergent slip increases truncation angles at halokinetic-sequence unconformities and creates cusps where they terminate against the salt (Fig. 7; Rowan et al., 2003; Giles and Rowan, 2012). Note that in all cases, the shear that occurs during folding is parallel to bedding rather than the edge of salt and has the opposite sense to that expected for a drag fold generated by relative salt rise and minibasin subsidence (Fig. 9d).

Two primary factors control the width of upturned collars of strata around diapirs (Rowan et al., 2003; Giles and Rowan, 2012). First is the thickness of the roof (Figs. 10a, b) because the wavelength of a fold depends largely on the thickness of the folded layer. Roof thickness is commonly determined by the interplay between salt-rise rate and sediment-accumulation rate: the higher the ratio between the two, the thinner the roof and thus the narrower the zone of drape folding. In general, sediment accumulation is greater in the minibasins than over the diapirs. However, an aggrading carbonate platform may generate a thick roof even at times of slow, marl-dominated deposition in the adjacent minibasins, as seen at Bakio diapir in the Basque Pyrenees (Rowan et al., 2012a; Poprawski et al., 2016; Roca et al., 2020). The second factor impacting the width of the upturned collar is the position on the topographic scarp where the salt

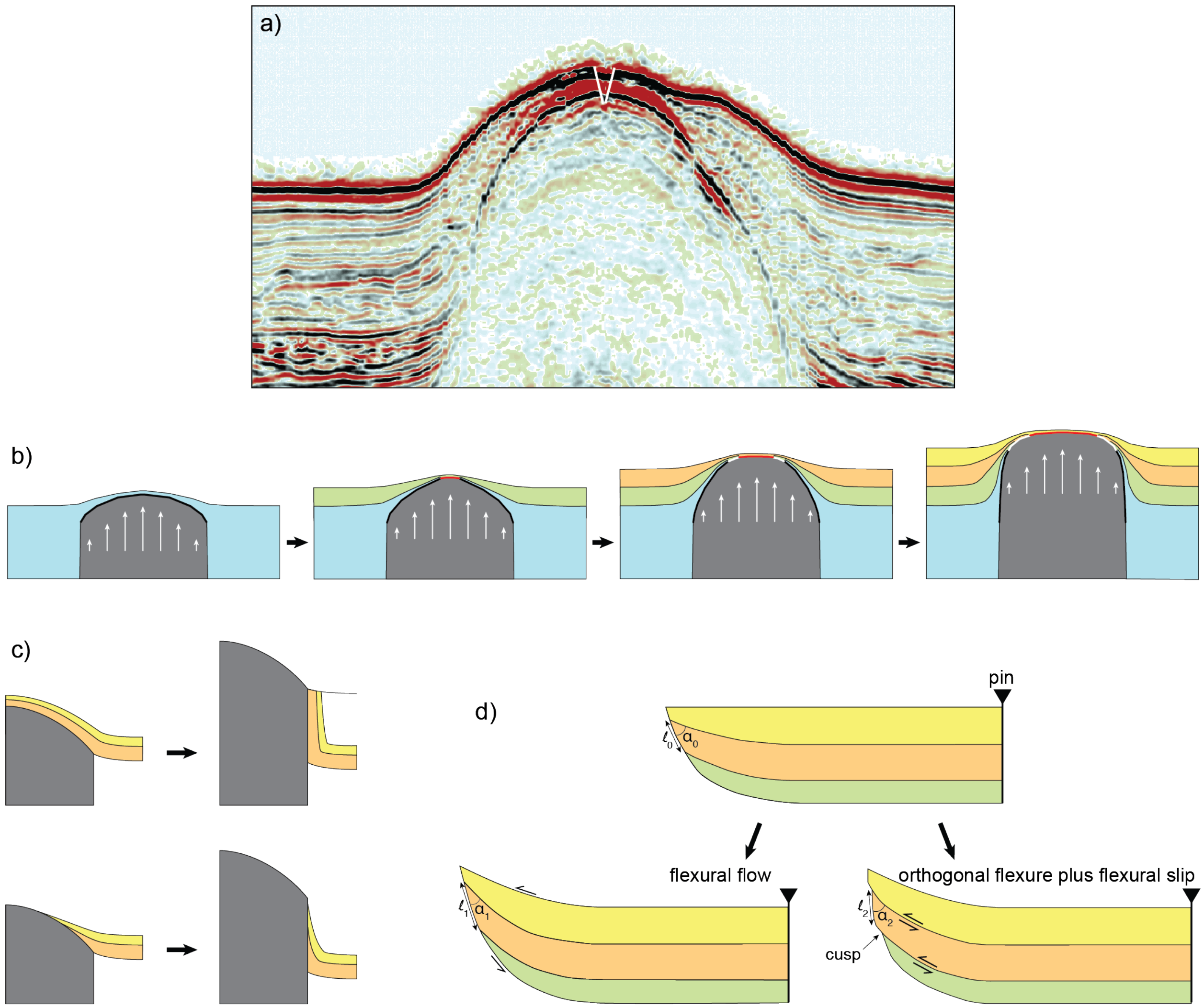

***Figure 9**. Drape folding over salt stocks/walls: a) 3-D time-migrated seismic line showing a diapir roof that is being separated by crestal faults (white) – the two flaps will end up on opposite sides of the diapir after further rise (no scale); b) schematic diagram showing progressively new roof that gets shouldered aside during salt rise (white arrows) so that the top salt ends up as the diapir edge (thick black line – original roof; thick red line – new roof at each stage; thick white line – new roof from earlier stages); c) schematic diagram showing concordant roof becoming ~parallel to the diapir edge (top) and onlapping roof ending up dipping less than the edge of salt (bottom); d) left – narrowing of wedge taper angle, decrease in cutoff angle ($\alpha_1 < \alpha_0$), and increase of cutoff distance ($\ell_1 > \ell_0$) during drape folding by flexural flow pinned in the minibasin (after Hearon et al., 2014); right – only minor changes in cutoff angle and distance (α_2 and ℓ_2 are almost equal to α_0 and ℓ_0) and creation of cusps in the salt-sediment interface in the case of orthogonal flexure of discrete competent beds (colored intervals) and flexural slip along thin weak levels (black lines).*

breaks out during further rise or lateral advance: if the diapir grows vertically, the entire width of the drape fold is preserved adjacent to the salt (Fig. 10c); base-scarp breakout results in no preservation of the folded strata next to or beneath the salt (Fig. 10d); and intermediate scenarios

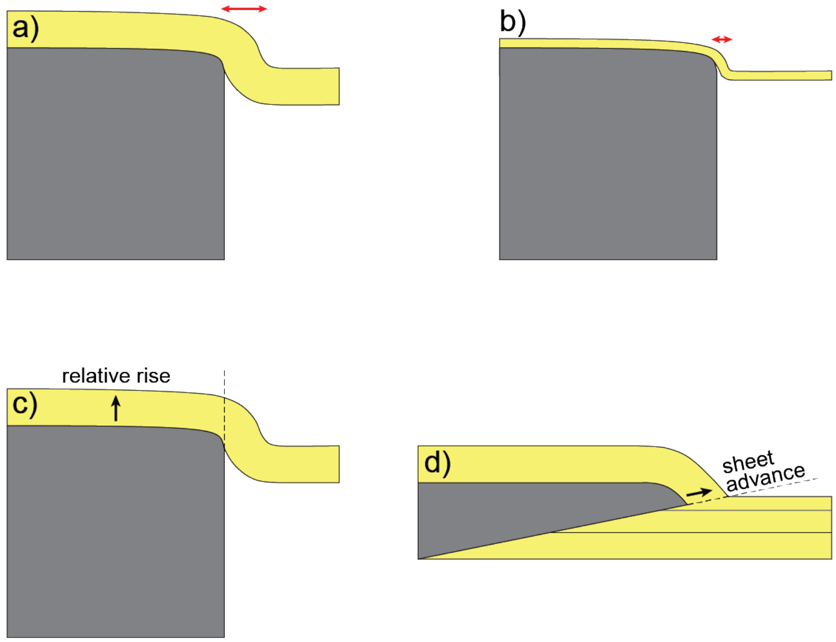

__Figure 10__. Controls on drape-fold width adjacent to salt: a) and b) roof thickness determines the width of the monoclinal fold (red arrows); c) and d) the trajectory of further salt rise or advance (black dashed lines) determines how much of the folded roof is preserved adjacent to or beneath salt. Yellow in (a) to (c) represents a single stratigraphic unit; yellow in (d) has no specific age connotation.

result in preservation of the lower portions of the drape fold. All of these factors that combine to control the width of the upturned collar vary with depth and over time so that the width fluctuates.

Halokinetic folds are relatively rare beneath salt sheets. Examination of eight sheets in South Australia reveals two examples where base-salt ramps are underlain by composite halokinetic sequences (Fig. 11a; Kernen et al., 2012; Hearon et al., 2015a; Rowan et al., 2019a). Also, the Salinas de Rosio salt tongue in the Basque Pyrenees has only a 10 m wide hook halokinetic sequence at its tip, similar to even smaller examples from the Sivas Basin (Fig.11b). The explanation depends on the type of salt sheet advance (see Hudec and Jackson, 2006, 2009; Hearon et al., 2015a; Rowan, 2017): in extrusive advance, in which the salt is exposed, there is no roof to fold; and in thrust advance, the salt typically breaks out at the toe of the scarp (roof-edge thrust of Hudec and Jackson, 2009) so that no subsalt fold is preserved (Fig. 10d). In the relatively uncommon cases in which the salt breaks out partway up a halokinetic drape fold (salt-roof thrust), some of the fold ends up preserved beneath the salt.

4.1.4. Collapse folds

In contrast to local halokinetic folds, where strata turn up toward the salt, strata may bend down toward the diapir over distances between 50 m to 1 km. These occur over the edge of the diapir top (Fig. 12a) or over salt shoulders (Fig. 12b, c). The presence of caprock and evaporite karst in the upper part of the Gypsum Valley diapir (Fig. 12b; see Giles et al., 2018, and

Langford et al., 2020) suggests that the folds formed due to dissolution collapse, although local evacuation of salt into the narrower part of the diapir or along strike may also play a role.

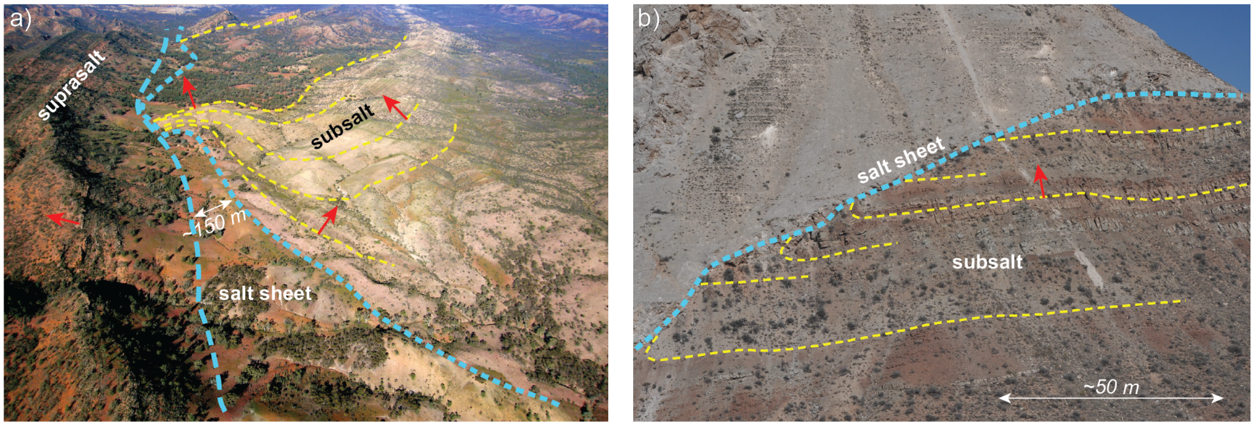

***Figure 11**. Drape folds beneath salt sheets: a) oblique aerial view of tapered composite halokinetic sequence in marine carbonates beneath a base-salt ramp in the Patawarta sheet, Flinders Ranges (modified from Hearon et al., 2015; see also Kernen et al., 2012); b) small hook halokinetic sequences in nonmarine redbeds beneath a salt sheet in the Sivas Basin (see Kergaravat, 2016; Kergaravat et al., 2017). Long-dashed blue is top salt, short-dashed blue is base salt, yellow is stratigraphic horizons, and red arrows indicate stratigraphic up.*

4.2. Seismic-scale faults

4.2.1. Faults associated with regional tectonics

Regional extensional, contractional, and strike-slip faults tend to terminate at and link salt stocks and walls. In cases where diapirs predate the onset of faulting, the weak salt again localizes the strain, getting widened, shortened, or sheared while the stronger minibasins are faulted. Alternatively, if the onset of regional deformation predates any salt movement, diapirs may subsequently nucleate along the faults, as in the classic case of extensional reactive diapirs that evolve into active and ultimately passive diapirs (Vendeville and Jackson, 1992). Similarly, salt glaciers may emanate from salt carried up in the hanging walls of emergent thrusts (Hudec and Jackson, 2006), or they emanate from counterregional faults that are in fact welded, leaning diapirs (e.g., Rowan, 2017). Salt sheets may also be modified by subsalt faults of various types (e.g., Hudec et al., 2009; Fiduk et al., 2016; Rowan, 2017).

Whatever the origin, faults may have different relationships to the edge of salt. In some cases, they appear to offset the edge, forming triangular cusps at the edge of salt (Fig. 5a). In others, they curve from their regional trends to terminate against the diapirs more orthogonally without any apparent offset of the diapir flanks (Fig. 13a). In yet others, they curve to become tangential to the salt-sediment interface, sometimes at tapered salt terminations (Fig. 13b).

In many cases, the faults appear to merge with the edge of salt (e.g., Figs. 5a, 13b) and indeed, many salt-sediment interfaces have been interpreted to be surfaces of slip (e.g., Kupfer, 1968;

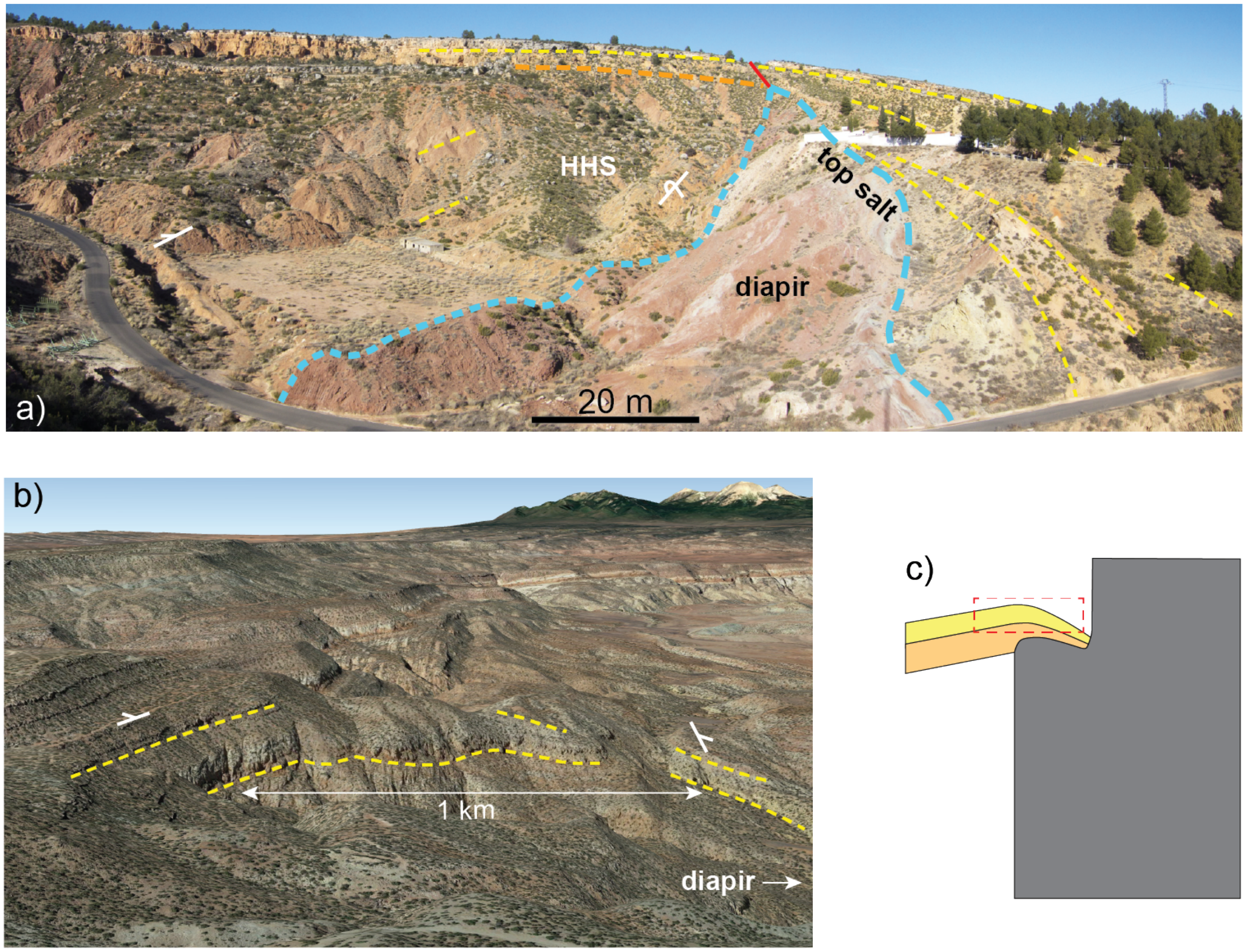

__Figure 12__. Collapse folds: a) Cofrentes diapir in the Prebetics of Spain, with a hook halokinetic sequence (HHS, with white showing bedding attitudes) flanking the edge of the diapir (short-dashed blue) and capped by an unconformity (orange), and a growth wedge (yellow) over the top of the diapir (long-dashed blue); b) GoogleEarth image of anticline in the Paradox Basin formed by minibasin strata dipping away from Gypsum Valley diapir (left) folded over to dip into the diapir (right) due to dissolution or evacuation of the underlying salt; c) sketch of portion of diapir (grey) with salt shoulder and strata folded down into diapir, with red box showing approximate location of image in (b).

Davison et al., 2000b; Alsop et al., 2000; 2016; Hearon et al., 2014). Whereas this appears to be the case at a seismic or regional scale, mechanical arguments suggest that it is not strictly correct, which has important implications for small-scale deformation adjacent to diapirs. There is increasing resistance to salt flow toward the edge of salt due to viscous drag effects (Fig. 2), so that it is easier to accommodate shear within the salt but at some, admittedly short, distance from the boundary. Therefore, although we have no field evidence to support this, we postulate that although the initial offset at any point that gets juxtaposed against the salt would be fault bounded, the relative movement quickly transitions to shear within the salt but very near its edge (Figs 14a, b). In other words, at any given time, there would be three components to the system

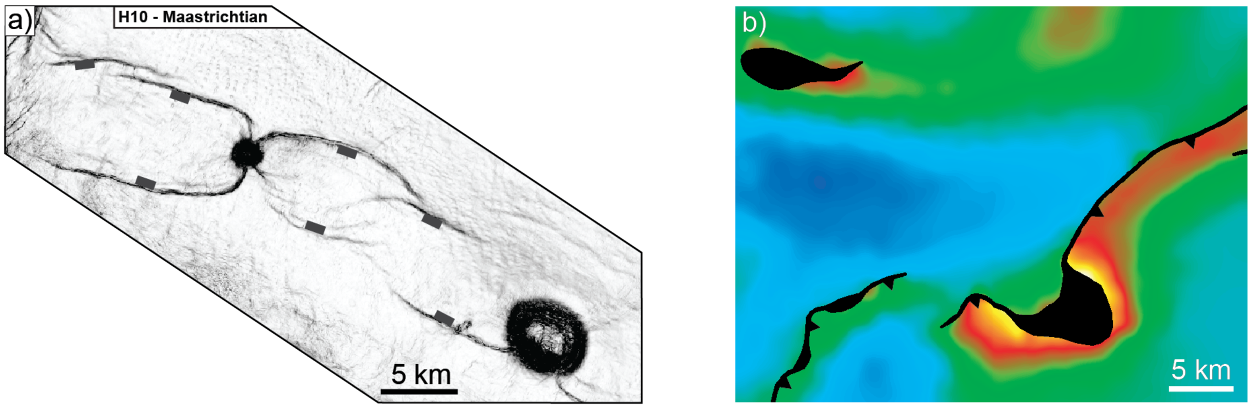

Figure 13. *Large-scale faults intersecting diapirs: a) seismic variance map showing suprasalt extensional faults in the Egersund Basin, Norway, curving to terminate against salt stocks (modified from Tvedt et al., 2016); b) depth-structure map showing salt-detached thrust faults in the northern Gulf of Mexico terminating against diapirs at tapered ends (modified from Rowan and Ratliff, 2012; colors indicate structural relief on a horizon, with blues being low and reds and yellows high). Diapirs shown in black.*

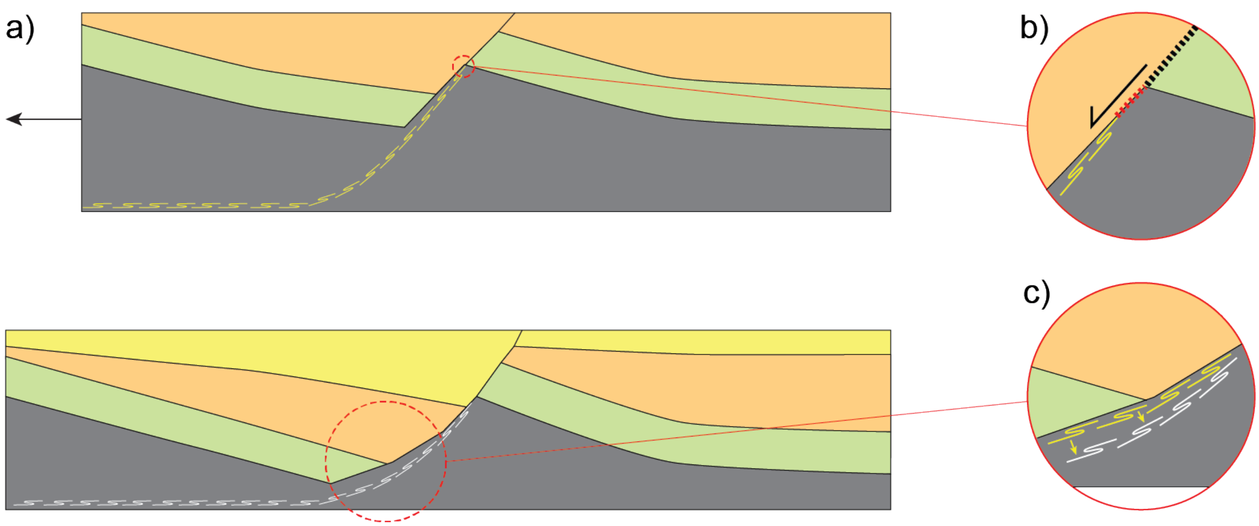

Figure 14. *Conceptual model for a fault transitioning to a shear zone just inside the edge of the salt (grey): a) two-step evolution of an extensional fault in the overburden and an intrasalt shear zone within the salt roller; b) close-up of where the fault merges with the salt (dotted black line is sediment-on-sediment fault; dotted red line is salt-on-sediment fault; yellow indicates intrasalt shear zone); c) close-up showing how the inner boundary of early shear (yellow) shifts into the salt (white) as the initial sliver of salt in the early hanging wall is thinned and stretched. The cartoons have no scale connotation and are not intended to show actual shear-zone thickness or details of salt flow.*

which accommodates displacement (Fig. 14b): a sediment-on-sediment fault away from the salt; a discrete fault at the salt-sediment interface, and an intrasalt shear zone. A thin sliver of salt behaves as a sheared part of the mostly sedimentary side of the intrasalt shear zone. As that sliver is progressively stretched and thinned, thereby becoming more resistant to shear, the inner boundary of the shear zone presumably shifts laterally, effectively accreting more salt into the near-edge shear zone (Fig. 14c). We envisage this process occurring with faults of any type, whether they accommodate regional extension (Fig. 14), contraction, or strike-slip, differential subsidence of minibasins, or near-diapir deformation .

Faulting associated with regional deformation does not necessarily increase in intensity toward the salt. However, there can be exceptions. For example, extending or squeezing a salt stock may lead to excess deformation in the flanking strata located in the regional strike direction, analogous to stress and strain concentrations around a hole in a metal plate that is extended or shortened (e.g., Savin, 1961). Examples include El Papalote diapir (Fig. 15a), where faults and local warping of bedding are concentrated at the northwestern and southeastern margins of the squeezed diapir (shortening was directed NNE-SSW), and Salinas de Rosio diapir in the Basque Pyrenees, where both early extensional and late contractional faulting is more pronounced at the strike margins.

4.2.2. Faults associated with minibasin-scale subsidence

Major faults formed due to differential vertical subsidence into salt also terminate against diapirs. The classic example is that of counterregional (landward-dipping) faults which form as deep salt moves into passive diapirs (e.g., Schuster, 1995; Diegel et al., 1995; Rowan and Inman, 2005). These faults extend away from and link salt stocks and salt walls, appearing to merge with the landward edges of the diapirs (Handschy et al., 1998; Trudgill and Rowan, 2004). Again, though, we suspect that the faults actually transition to intrasalt shear zones near the salt-sediment interface. Counterregional faults merge with the ends of the longitudinal edges of salt walls in the Paradox Basin (Escosa et al., 2018; Thompson Jobe et al., 2019), but the outcrop quality is inadequate to resolve the detailed geometry.

4.2.3. Faults associated with folding

Any type of folding may, of course, be accompanied by brittle faulting that is large enough to be imaged on seismic data. This includes near-diapir drape folding in local halokinetic sequences, in collapse folds, and in megaflaps. We address in turn radial and diapir-parallel faults induced by drape folding or collapse adjacent to or above, respectively, stocks and walls.

Field exposures, like subsurface data (e.g., Davison et al., 2000a), show that radial faults are most common around salt stocks and at the ends of salt walls (Figs. 15a-c). These are extensional faults roughly perpendicular to the salt-sediment interface that commonly terminate against the salt at cusps. They may extend out less than 1 km, i.e. no farther than the limit of halokinetic drape folding (Fig. 15a), or they may have longer lengths when the zone of near-diapir folding is wider, for example in the case of contractional squeezing of the salt (Fig. 15b) or megaflaps (Fig. 15c, southeastern end).

The radial faults illustrated in Figures 15a-c can all be attributed to hoop stress related to folding of strata above and adjacent to diapirs. But can they also be generated by lateral

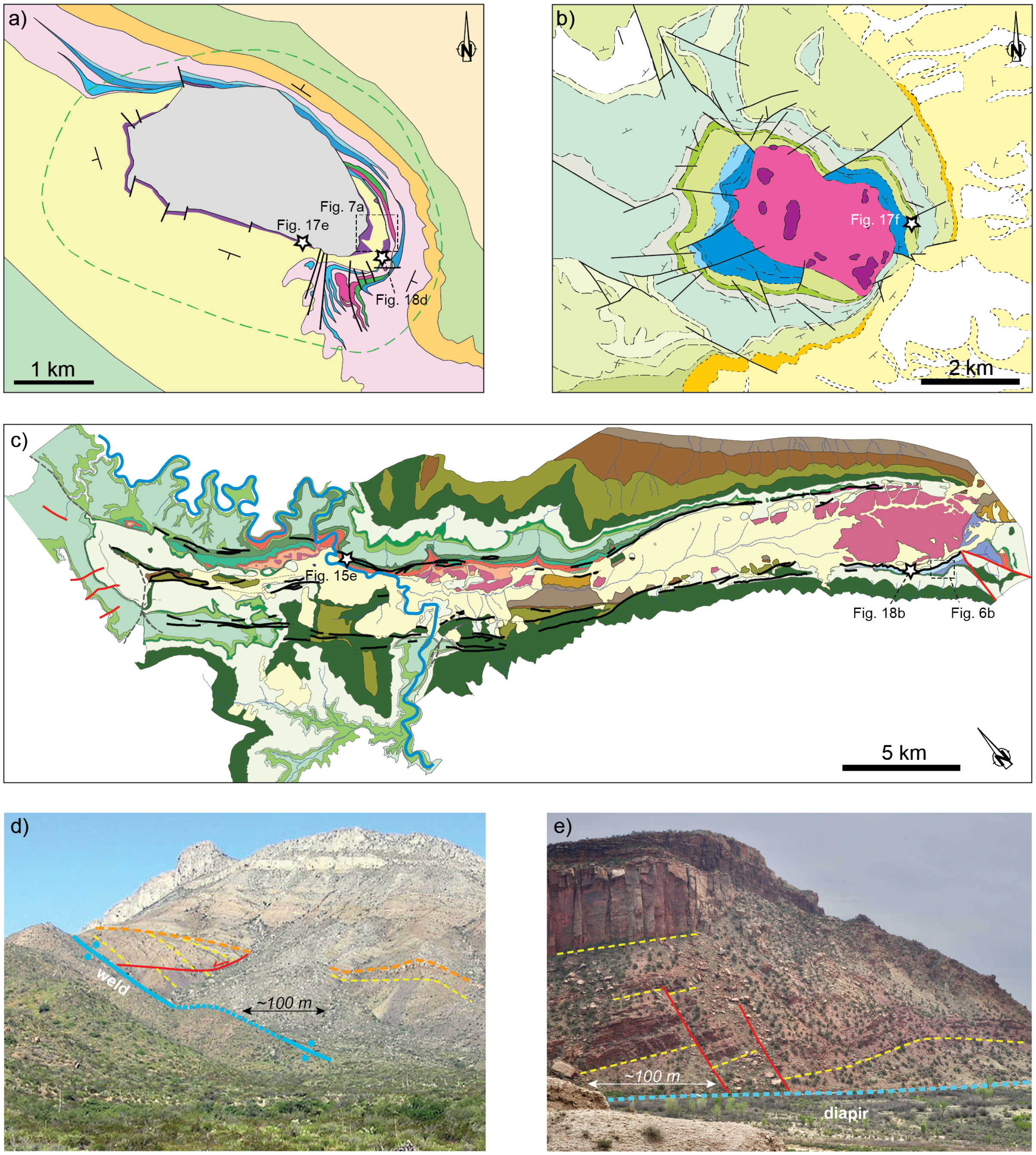

***Figure 15**. Faulting around diapirs: a) radial faults at El Papalote diapir (grey), La Popa Basin, extending no farther that the limit of halokinetic drape folding (green dashed line) (modified from Rowan et al., 2003); b) radial faults at Poza de la Sal diapir (pink), Basque Pyrenees, that extend multiple km from the diapir due to contractional doming (modified from Quintà et al., 2012); c) Gypsum Valley diapir (pink and pale orange), Paradox Basin, with diapir-parallel faults (black) similar to those in (e) along the length of the salt wall and radial faults (red) at both ends (modified from Escosa et al., 2018); d) diapir-parallel growth fault (red) terminated upward at halokinetic-sequence unconformity (orange) and rotated to subhorizontal by drape folding at the vertical La Popa weld (modified from Rowan et al., 2012b); e) diapir-parallel collapse faults (red) above salt shoulder at Gypsum Valley diapir, Paradox Basin (location shown in (c)).*

expansion of the salt into the minibasin strata (stem push), as suggested by numerical models (Luo et al., 2012; Nikolinakou et al., 2014; Heidari et al., 2017) and interpreted in the subsurface (Coleman et al., 2018)? We argue that the field data do not support this interpretation. First, most faults do not extend beyond the zone of near-diapir folding (Figs. 15a-c), in contrast to model faults caused by stem push. Second, when they do, we suggest that an applied regional stress field has reactivated those radial faults with appropriate orientations. For example, in the Santos Basin, radial faults that extend beyond the limit of drape folding (Coleman et al., 2018) have two dominant trends that also exist in minibasins between the diapirs, and roof strata well above regional imply some contractional deformation. A similar situation occurs in the Espírito Santo Basin (Mattos and Alves, 2018; Maunde and Alves, 2020). Third, we find no field evidence, in the form of mesoscale structures or microscopic fabrics, of the shortening required if diapirs are expanding into the minibasins. Nor do we see any apparent reduction in sandstone porosity due to lateral compaction close to diapirs.

Seismic-scale diapir-parallel faults are more common along the lengths of salt walls than around salt stocks (e.g., Fig. 15c). We attribute some of these extensional faults as well to folding of strata above and adjacent to diapirs, generated by bending stresses and outer-arc extension during drape folding. The large faults most commonly dip inward toward the diapir and get rotated along with the roof strata during drape folding until they attain low-angle to subhorizontal dips close to the salt (Fig. 15d; Hennessy, 2009). If the faults dip outward, they rotate into steep or even overturned attitudes. In either case, large-scale faults in halokinetic drape folds are relatively rare, and it may be that the roof typically breaks only at the crest of the diapir (depending on the shape of the top salt), such that flaps without major faults rotate as the diapir continues its rise (Fig. 9a).

Diapir-parallel faults may also form during collapse of suprasalt strata into the top of the diapir or a salt shoulder due to dissolution or salt evacuation into another, still growing part of the diapir. These have relatively steep dips toward the salt and often occur in arrays that drop the overburden progressively down into the salt, with or without accompanying folding (Fig. 15e).

4.3. Small-scale deformation

In this section, we describe sub-seismic-resolution features adjacent to stocks and walls and beneath salt sheets. We address first brittle structures ranging from small-scale faults to opening mode fractures to deformation bands, then small-scale folds, and finally fabrics such as shear zones or other foliations. Our examples are exclusively from outcrops and we focus solely on small-scale structures associated with the salt growth/emplacement itself rather than those that have regional distribution (see later Discussion).

4.3.1. Brittle structures

Small-scale faults and other fractures are not characteristic features of strata adjacent to diapirs or beneath sheets. There are many examples of near-diapir or subsalt strata with no or only regional small-scale deformation (Fig. 16). When they do exist, the most common structures adjacent to stocks/walls are opening-mode veins and extensional faults with millimeter- to

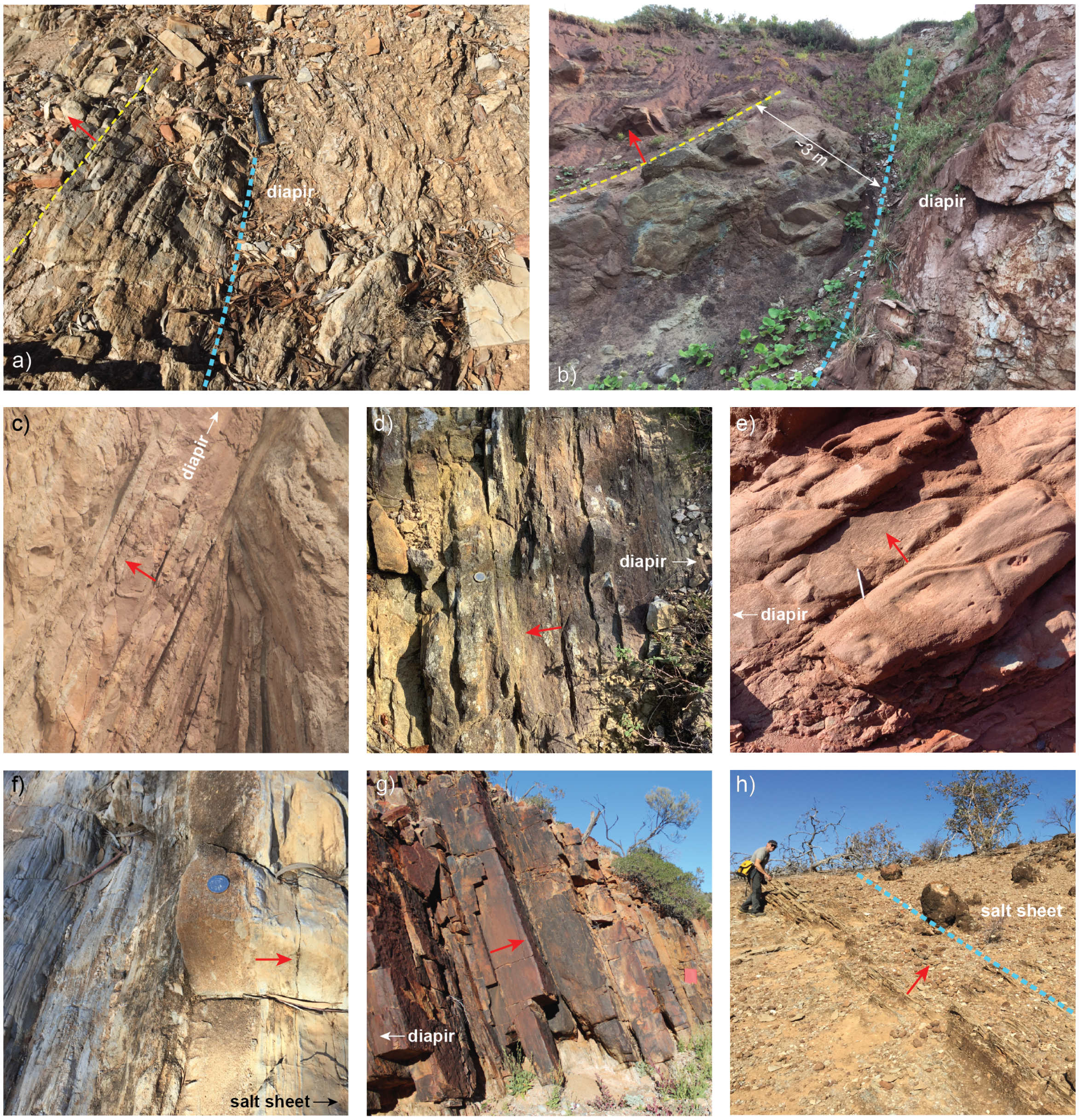

Figure 16. *Near-salt beds with no or only regional fractures (blue is salt-sediment contact, red arrows are stratigraphic up): a) contact between Apex Hill diapir, Flinders Ranges, and flanking dolostones (hammer for scale); b) contact between Finlay Pt. diapir, Nova Scotia, and flanking conglomerate which has fabric parallel to bedding, not the edge of salt, whereas the gypsum has internal flow fabrics; c) limestones within ~20 m of edge of Ilcheh diapir, Zagros Mts. (no scale, location shown in Fig. 7c); d) fluvial sandstones in vertical flap 100 m from Villasana de Mena diapir, Basque Pyrenees; e) fluvial sandstones within ~30 m of Onion Creek diapir, Paradox Basin; f) dolostones within 10 m of Apex Hill diapir, Flinders Ranges; g) quartzites in megaflap 100 m from Witchelina diapir, Willouran Ranges, South Australia (location shown in Fig. 6a); h) dolostones just beneath Arkaroola salt sheet, Flinders Ranges.*

decimeter-scale offsets that strike parallel to the edge of salt. The faults commonly form conjugate sets with respect to bedding, with the acute bisector perpendicular to bedding, but may also comprise arrays that dip predominantly away from the diapir (Figs. 4e, 17a, b). Thus, they record early layer-parallel extension: the conjugate sets probably formed when the roof strata were subhorizontal and just starting to be folded over the rising diapir; and the outwardly dipping fault sets likely formed slightly later when the strata were dipping somewhat more steeply. But the amount of extension is almost never significant. In the Witchelina megaflap of South Australia (Fig. 6a), for example, where the strata reach vertical to slightly overturned, extension is locally up to 7% (Canova, 2017), but a qualitative assessment attained from examination of the entire 2.5 km high megaflap suggests at most 1-2% bed lengthening (see Fig. 16g). This is typical of the other megaflaps and halokinetic sequences in each of the salt basins that we have examined.

Other diapir-parallel fractures may develop due to outer-arc extension in drape folds formed by orthogonal flexure, especially in brittle carbonates in tight hook halokinetic sequences. Small-scale faults and opening-mode fractures are associated with larger-scale collapse faults, for example those caused by dissolution of underlying salt (Fig. 17c). A unusual type is shown in Figure 17d, where en-echelon veins at the diapir margin suggest an unexpected minibasin-up sense of shear, the opposite of that expected for diapir rise. They likely formed during sand-on-sand flexural slip on a halokinetic sequence-bounding unconformity, with the sandstone subsequently getting juxtaposed against the salt during ongoing drape folding and concentrated slip on the unconformity (see Rowan et al., 2003, figs. 7 and 8). Other fractures and small-scale faults around diapirs are radial, similar to the larger-scale radial faults that form due to hoop stress where there is map-view curvature of the salt-sediment interface (Fig. 17e).

Deformation bands adjacent to exposed diapirs are also rare and localized in our experience. For example, pervasive granulation seams are found on one flank of one diapir in Nova Scotia (Alsop et al., 2000) but we did not observe any significant development adjacent to other nearby diapirs. At Poza de la Sal diapir, a fluvial sandstone approximately 150 m from the salt edge is undeformed in one area but is intensely deformed just 40 m along strike adjacent to a major radial fault (Fig. 17f).

In the case of salt sheets, small-scale subsalt brittle structures are rare to absent (Fig. 16c) except where there are halokinetic folds. In these cases, we observe the same types of faults and other fractures as in halokinetic sequences flanking steep diapirs: diapir-parallel extensional structures accommodating minor bed lengthening and similarly oriented fractures due to outer-arc extension during folding. Although we have no examples, we also expect radial faults/fractures in subsalt halokinetic drape folds due to hoop stress if there is map-view curvature of the front of the salt sheet.

4.3.2. Small-scale folds

Folds that are below seismic resolution adjacent to salt stocks and walls have several possible origins. First, the most common are those that form during soft-sediment deformation within

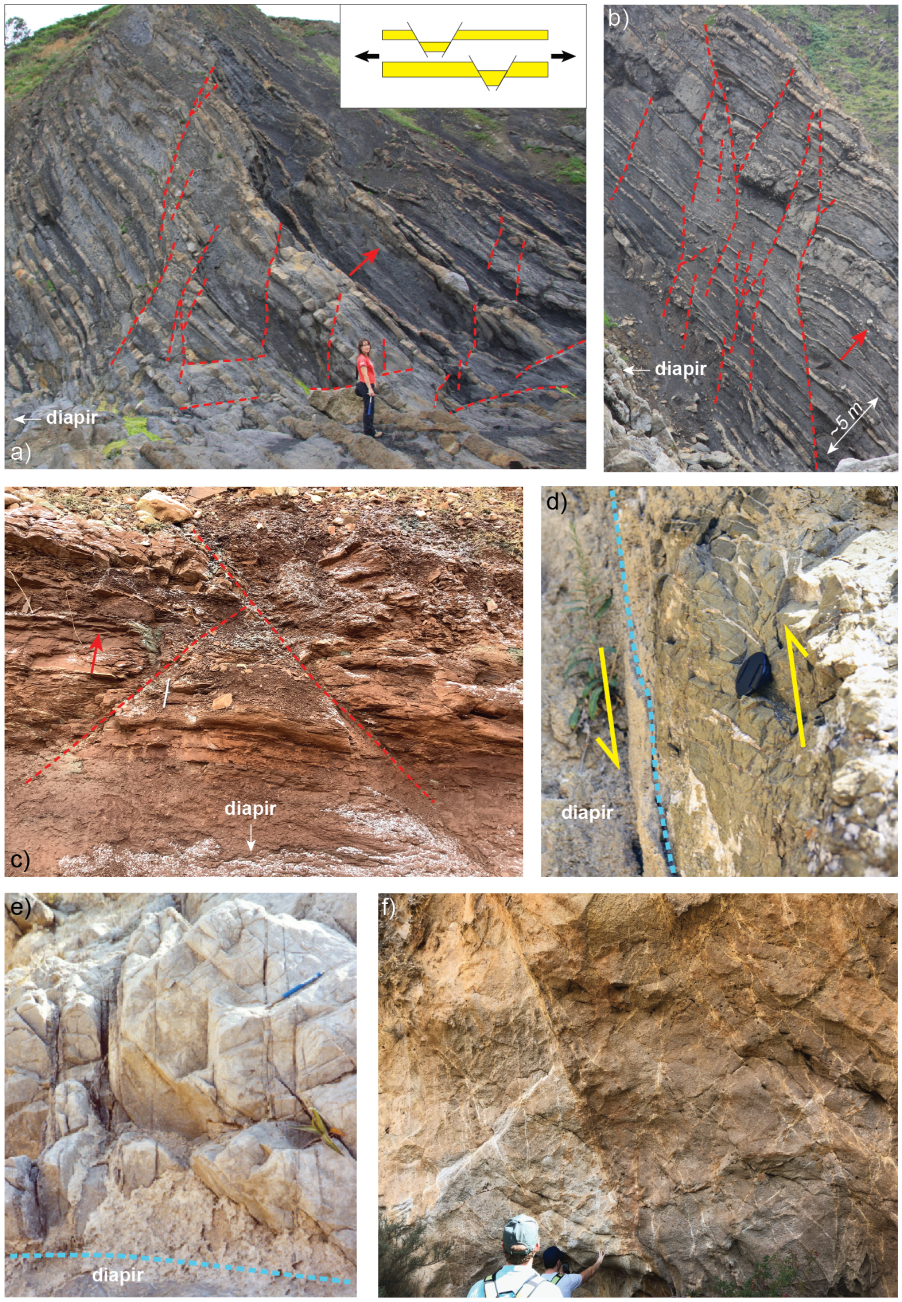

Figure 17. *Small-scale brittle deformation adjacent to diapirs (red arrows are stratigraphic up): a) conjugate set of faults accommodating very early bed lengthening of marls and calciturbidites adjacent to Bakio diapir, Basque Pyrenees (location shown in Fig. 7e; inset shows symmetric faults caused by extension of horizontal beds); b) faults with dominant dip away from Bakio diapir (location shown in Fig. 7e); c) extensional faults in nonmarine sandstones due to collapse above Onion Creek diapir, Paradox Basin; d) en-echelon veins in tidal sandstone adjacent to La Popa weld, La Popa Basin, showing minibasin-side up sense of movement (yellow arrows); e) radial veins in vertical limestone next to El Papalote diapir, La Popa Basin (location shown in Fig. 15a); f) deformation bands seen at base of vertical fluvial sandstone in damage zone of nearby larger radial fault at Poza de la Sal diapir, Basque Pyrenees (location shown in Fig. 15b).*

discrete mass-wasting deposits (Fig. 18a). Second, asymmetric folds may form due to flexural flow during drape folding, as observed in strata adjacent to Poza de la Sal diapir. Third, squeezing of a diapir with a thin roof may generate short-wavelength folds that subsequently rotate to steeper attitudes in halokinetic folds, as observed adjacent to La Popa weld (Fig. 18b). We have observed no examples of folds within diapir-flanking strata with a shear sense compatible with drag induced by diapiric rise.

Small-scale folds are also typically rare beneath salt sheets. They have been reported from Yemen and attributed to shear beneath an advancing salt glacier (Davison et al., 1995, 1996). Similarly, folds beneath a partly welded sheet in South Australia were thought most likely to have formed during salt emplacement, although tectonic or synsedimentary origins could not be eliminated (Williams et al., 2019). A reevaluation of these folds, however, shows that they extend for multiple km beneath the salt and formed during later orogenesis (see Discussion section). Examination of eight exposed salt sheets in South Australia reveals no small-scale subsalt folds other than those related to soft-sediment deformation or regional tectonic deformation.

4.3.3. Shear zones/fabrics

Planar fabrics and shear zones are also rare adjacent to stocks/walls and beneath salt sheets. However, there are a few exceptions. First, a 1-3 cm wide shear zone exists in at least one location along the salt-sediment interface at Bakio diapir in the Basque Pyrenees (Fig. 18c). However, the contact here is between an intrasalt volcanic stringer and flanking marly limestones, so this is not the typical scenario of weak salt juxtaposed against relatively strong sediment. Second, as already stated, very narrow zones of shear adjacent to diapirs and beneath sheets have been reported in the gypsum-dominated Sivas Basin (Kergaravat, 2016; Collon et al., 2016; Kergaravat et al., 2017). Third, cataclastic shear also occurs along a halokinetic unconformity at El Papalote diapir (Fig. 18d) and minor shear fabrics are found within vertical mudstones parallel to the La Popa weld (Fig. 18e). Both of these examples record diapir-down senses of movement, but were caused instead by flexural slip/flow during halokinetic drape folding. In summary, the usual lack of any diapir-flanking or subsalt shear zones suggests that relative movement of salt and surrounding sediments is accommodated primarily, if not exclusively, by intrasalt shear.

A massive breccia beneath a salt sheet in the Prebetics of Spain (Fig. 18f) might be considered as a subsalt shear zone. However, there is no structural fabric and the breccia contains clasts of both diapir and roof material but not subsalt minibasin strata. Thus, we interpret it as slumped carapace subsequently overridden by the salt. We suggest that this is, in most cases at least, a better explanation for the subsalt rubble zones penetrated by wells that have been attributed by some to shear or drag related to lateral salt flow.

***Figure 18**. Small-scale ductile deformation adjacent to diapirs: a) isoclinal fold pair in mass-transport deposit interbedded with turbidites flanking Bakio diapir, Basque Pyrenees; b) oblique view of short-wavelength folds in overturned limestone truncated by a halokinetic-sequence unconformity overlain by beds dipping vertically away from the viewer (La Popa weld, La Popa Basin; modified from Rowan et al., 2012b); c) 1-3 cm wide zone of sheared marls (black) at contact with igneous stringer within Bakio diapir, Basque Pyrenees (upper left); d) cataclastic shear zone along halokinetic unconformity at El Papalote diapir, La Popa Basin (location shown in Fig. 15a); e) diapir-parallel shear accommodating flexural slip during drape folding of fluvial mudstones at La Popa weld, La Popa Basin; f) boundary between Keuper salt sheet and underlying breccia and marls in the Prebetics, SE Spain. Bedding in yellow; unconformity in orange; base salt in blue; intrasalt boundary in black; red arrows show stratigraphic up; black arrows show sense of shear; white lines in (d) show shear (S) foliation.*

5. Discussion

5.1. Exceptions

Examination and analysis of exposed passive salt structures show that most near-diapir deformation is caused by drape folding of roof strata. As such, there is usually relatively minor development of faults and fractures adjacent to salt stocks and walls or beneath salt sheets – no more than is typical for any folded strata. However, there are numerous exceptions, with the most common occurring when there is regional deformation such as tectonic or gravity-driven extension or contraction. This generates larger-scale faults and folds, with their associated small-scale structures, that may impact the diapirs and their flanking strata. It can be difficult, however, to distinguish between structures caused by regional stresses and those caused by salt flow during diapir rise or sheet emplacement (see below).

Even when there is regional deformation, there is typically little associated deformation around the salt because the strain is preferentially accommodated within the weak salt. For example, salt-detached thrust sheets in fold-and-thrust belts such as the Pyrenees and Prebetics of Spain or the Kuqa foreland basin have minimal to no subsalt deformation even though relative displacement may be an order of magnitude greater than in passive diapirs. If, however, a diapir or sheet becomes welded and there is subsequent weld-parallel slip, flanking strata can be sheared and fractured (Figs. 19a, b), just as with any fault. The damage zone can be exceptionally wide, which may be due to irregularities in the two edges of salt that become juxtaposed to form the ‘fault’ (Rowan et al., 2012b).

A common scenario makes it even more difficult to identify just how much deformation is caused directly by salt flow in passive diapir rise or sheet emplacement. We have suggested that faults that appear to offset the salt actually transition into shear zones just within the salt (Fig. 14), in which case no associated deformation of the flanking sediments is expected. However, damage zones generated by slip between relatively strong rocks away from the salt may end up juxtaposed against the salt and thus be misinterpreted as being caused by salt flow. These faults may be regional extensional faults (Fig. 20a), contractional faults (Figs. 20c), or strike-slip faults. In the case of Figure 20c, it is unclear whether the subsalt deformation was generated by thrusting in front of the advancing salt, which had a minimum of 1.5 to 2 km of overburden at the onset of deformation, or by shear of the highly deformed igneous stringer just above the base salt. Another possible example is provided by the diapirs on Cape Breton Island, Nova Scotia, which were growing during a time of regional transpression (e.g., Waldron et al., 2015), so that major thrust and wrench faults connected the diapirs. At least some of the deformation attributed to diapirism (Alsop et al., 2000) is thus likely to have been related instead to regional tectonics. This is compatible with our own examinations of the same diapirs, in which we observed little small-scale deformation in halokinetic folds but more when there was clear evidence of shortening. Strata currently flanking the salt may have been deformed away from the salt (analogous to Fig. 19a, but in a strike-slip or contractional setting).

Figure 19. *Exceptional small-scale deformation adjacent to salt: a) brecciated sandstone in broad shear zone within 3 m of La Popa weld, La Popa Basin; b) highly sheared and fractured marls in the hanging wall of the Sopela incomplete thrust weld, Basque Pyrenees (blue is edge of salt, red arrow shows overall thrust sense, yellow arrows show shear within flanking strata); c) conjugate sets of fractures 250 m beneath salt sheet in Willouran Ranges, South Australia; d) enhanced orogenic cleavage 5 m beneath tertiary weld in Willouran Ranges; e) intense fracture development and mineralization ~50 m beneath Arkaba salt sheet, Flinders Ranges, South Australia; f) conjugate faults, en-echelon veins, and cleavage (S_1) locally developed 10 m from edge of Bakio diapir, Basque Pyrenees.*

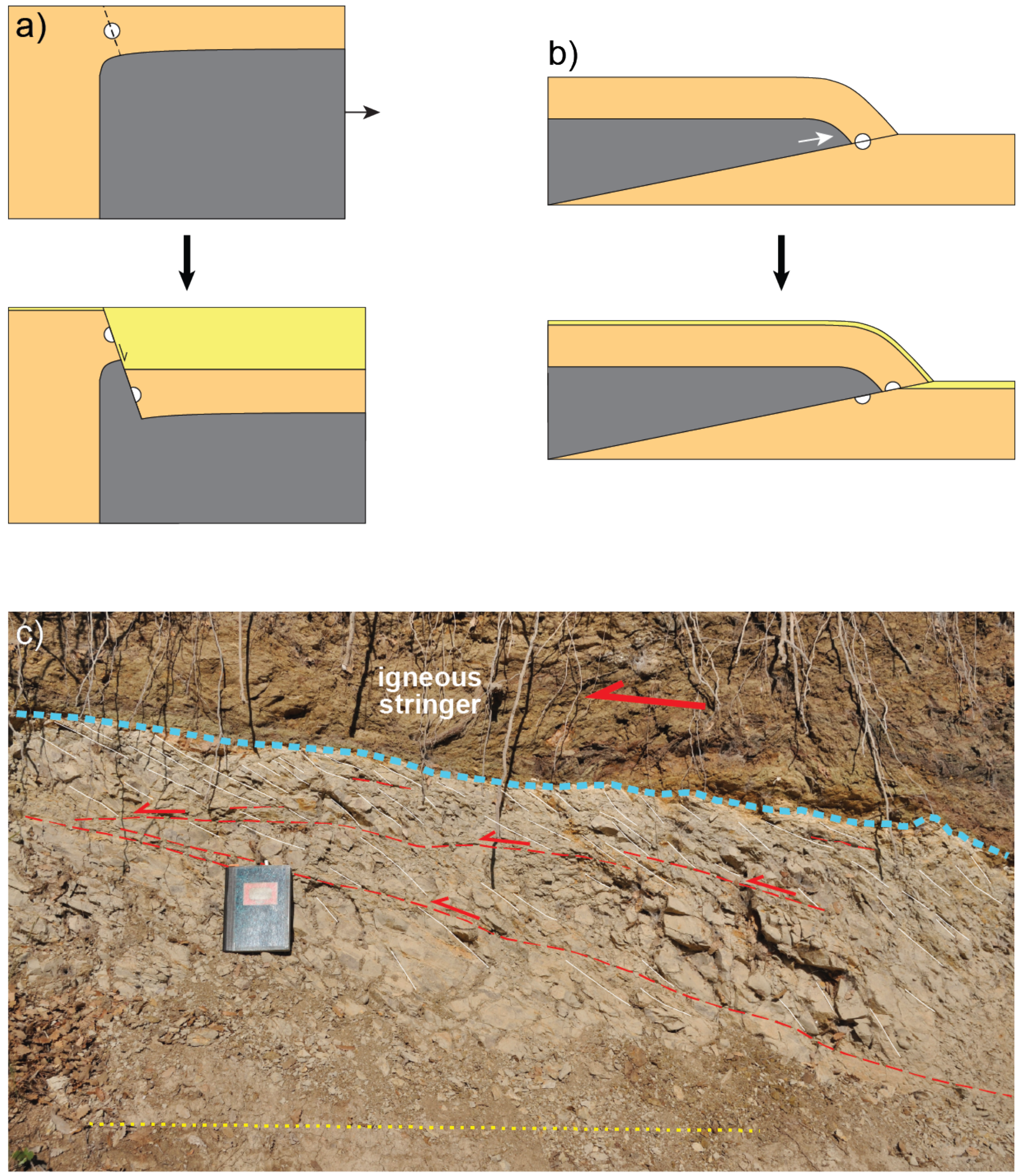

Figure 20. *Juxtaposition of damage zones next to salt: a) and b) extensional collapse of buried diapir and thrust advance of salt sheet, respectively (both in grey) – in each case, areas originally across the faults from each other (whole circles) get offset, with one side (half circles) ending up adjacent to the salt; c) sheared marls in footwall of salt-bearing thrust in Catalan Pyrenees (with ~40 km of displacement) that may have formed early, in front of the advancing thrust (as in (b)), or due to emplacement of highly deformed igneous stringer (blue is base salt, red lines are minor thrusts/shears, red arrows show thrust sense, white lines indicate shear foliation, yellow dotted line is approximate bedding orientation from areas outside of photo).*

Juxtaposition of damage zones generated away from salt into positions adjacent to salt may also occur during passive diapir growth or sheet emplacement in the absence of regional tectonic deformation. The roofs of some passive diapirs are offset by faults that appear to merge with the edge of the rising salt (Hearon et al., 2014) and, as mentioned earlier, many salt sheets are emplaced by thrust advance (Hudec and Jackson, 2006) in which a thrust fault links the tip of the sheet to the sea floor. Fault-related damage that originated above or in front of the salt can be mistaken for deformation caused by the salt movement itself (Fig. 20b). This is especially likely if the roof comprises stronger rocks, such as old carbonate carapace above canopies in the Gulf of Mexico (Fiduk et al., 2014), that advance over young, weak sediments, thereby potentially generating small-scale structures within the weaker strata that end up beneath the salt sheets.

Another example of regional deformation generating what might be mistaken for purely salt-related deformation is in the Willouran Ranges of South Australia. There, a combination of folds, veins, joints, and cleavage (Figs. 20c, d) is found beneath a partly welded subhorizontal salt sheet. However, we see no increase in fold development or fracture/vein intensity with increasing proximity to the base salt (see also Williams et al., 2019) – the folds exist throughout the entire subsalt minibasin and the fractures occur in swarms dispersed over at least 500 m of subsalt strata (e.g., Fig. 19c). Our analysis shows that there are two internally consistent sets of small-scale structures and orogenic cleavage that indicate first sinistral and then dextral transpression. Interestingly, cleavage intensity is greater just beneath the welded portion of the sheet (Fig. 19d) than elsewhere, possibly due to the lack of weak salt to accommodate some of the contractional strain.

There can be other causes of anomalous deformation adjacent to salt. First, subsalt strata beneath the Arkaba salt sheet in the Flinders Ranges display brittle structures that increase dramatically in intensity up-section toward the base of salt. In an area about 30-50 m beneath the salt, the siliciclastic beds are effectively shattered, with secondary minerals along bedding and along fractures with various orientations (Fig. 19e), including tablet boudinage within bedding. We suggest that this unusual deformation represents hydraulic fracturing by overpressured fluids, with the pressure probably controlled in part by the relatively impermeable salt sheet just above.

Second, another example of anomalous deformation occurs in marls on the east side of the Bakio diapir in the Basque Pyrenees. There, an internally consistent set of conjugate faults, en-echelon veins, and cleavage (Fig. 19f) records σ_1 (the principal compressive stress) that is oriented down the dip of bedding, which is overturned and parallel to the edge of the salt. This is very local and is the opposite of the pattern on the other side of the diapir, where there is only minor lengthening down the dip of the flanking strata (Figs. 17a, b). Moreover, it does not fit either the stress regime expected during diapirism or that related to the later Pyrenean shortening. The anomalous features occur just beneath a massive carbonate breccia with an irregular base, and we therefore attribute the local intense deformation to buttressing of flexural-slip against the base of the megabreccia during drape folding.

Third, a different type of unusual near-diapir deformation is observed on the north side of Onion Creek diapir in the Paradox Basin, where there is a salt shoulder between the exposed, inner part of the diapir and the edge of the flanking minibasin (Lankford-Bravo et al., 2019). Above the shoulder is a series of short-wavelength, tight growth folds with occasional thrusts.

The chevron geometries imply a contractional origin, but there was no known regional shortening at the time. Instead, the structures probably developed by outwardly directed gravity gliding of the thin roof above the shoulder, buttressed against the thick, strong minibasin (Lankford-Bravo et al., 2019).

All the examples described above illustrate that locally, unusual stress configurations may result from different causes. They may impact the amount of deformation in rocks adjacent to stocks and walls and beneath sheets, but we emphasize that these are the exceptions rather than the norm.

5.2. Origin and timing of deformation

As emphasized above, one of the greatest difficulties in trying to understand near-diapir deformation is distinguishing between deformation caused by passive diapirism (stock/wall growth or sheet emplacement) and that generated by other causes such as regional tectonics and associated other styles of diapirism (e.g., early reactive stage or late rejuvenation). Overprinting or cross-cutting relationships can be useful, but they only record the relative ages of two different episodes of deformation, not their absolute ages or origins. However, differentiating between multiple deformation events is sometimes a tractable problem when appropriate data are available. For instance, paleofluid analysis of vein fill might show high temperatures or isotopic values indicative of orogenic or metamorphic origins (e.g., Evans and Battles, 1999; Anderson et al., 2004), especially if the data match those of a known regional orogenic event that postdated the age of the near-diapir rocks being evaluated. Examples include the Cambro-Ordovician Delamerian Orogeny that affected the Neoproterozoic syndiapiric rocks of the Flinders Ranges and the Upper Cretaceous to Cenozoic Pyrenean Orogeny that impacted older Cretaceous growth strata around diapirs.

The problem becomes yet more difficult when passive diapirism was coeval with regional deformation. This might be orogenic, as in the case of the Nova Scotian, Pyrenean, or Kuqa diapirs, but it is even more common on passive margins such as the Gulf of Mexico, where gravity-driven deformation was typically ongoing while salt stocks were growing and sheets were being emplaced. Similarly, coeval extension and passive diapirism was common in many global salt basins.

One possible tool in all cases, regardless of timing, is standard structural analysis of the observed deformation, although this typically involves some assumptions. For example, faults and opening-mode fractures that have consistent geographic orientations around a circular salt stock imply an origin other than passive diapir growth, in which the structures would be expected to be axially symmetric (e.g., Quintà et al., 2012). If growth strata and local unconformities indicate that near-diapir folding was syndepositional, then fractures compatible with the larger-scale folds mostly likely formed during halokinetic drape folding. Or we can assume that the stresses associated with sheet emplacement are controlled by the direction of advance, which can sometimes be determined from the three-dimensional geometry of the sheet or from the orientation of the associated drape fold (see Hearon et al., 2015a). Thus, if the observed structures deviate significantly from this expected pattern, there is reason to suspect, but admittedly no proof, that they had a different origin. Another scenario is when small-scale faults, veins/fractures, and folds have orientations internally consistent with an associated regional orogenic cleavage, in which case they are likely to be orogenic as well rather than related to passive diapirism or sheet emplacement (unless the two stress systems were parallel).

In any case, a key element in such structural analyses is to move away from the stocks/walls and sheets and to first establish the regional, background levels and styles of deformation. Of course, there can be many reasons for spatial variations in the style, orientation, distribution, and intensity of deformation (the deformation pattern of Fischer and Jackson, 1999), but if there are no significant changes with increasing proximity to the salt, then the structures are unlikely to have been related to passive diapirism or sheet emplacement. Even if there are pronounced and systematic changes as the salt is approached, it can still be difficult or impossible to determine whether the deformation was generated by passive diapirism/sheet emplacement or some later external event, with the presence of salt influencing the structures that develop.

A more subtle, but critical, approach is to focus not on the deformation but on the lack of deformation. Structural geologists have a natural tendency to concentrate on, and give more weight to, cases with significant deformation. But evidence of a lack of small-scale deformation is at least as important, especially if it is the norm. If, out of eight salt sheets for example, two have notable subsalt deformation but six have pristine subsalt strata, then conceptual models should be based on those six. The question then becomes why the other two are exceptional. The possible causes to be considered include regional deformation, increased pore pressure, hydraulic fracturing, or more unique situations (as in the examples of Fig. 19).

5.3. Models vs empirical data

Analog models can reasonably mimic large-scale geometries and processes, but they cannot address small-scale deformation adjacent to salt stocks/walls and beneath sheets. Numerical models, on the other hand, have been applied in an attempt to understand and predict the stress and resulting strain near diapirs and sheets (as summarized above). However, as shown in this review, it is striking that although the models generally predict large amounts of deformation, this is rarely what we observe in the rocks.

One likely explanation for this mismatch lies in the material properties used in the models, which entails two components. First, most of the recent models of near-salt deformation are based on soil-mechanics models in that they assume cohesionless elastoplastic or poroelastoplastic behavior for the surrounding sediments, which effectively replicates homogeneous and isotropic, weak, unconsolidated mudstones (see review by Nikolinakou et al., 2018a). Yet real minibasin strata are stronger, especially at depth, and the presence of faults at the sea floor over diapirs in basins like the Gulf of Mexico (Fig. 9a) shows that even very shallow roof sediment has more strength than commonly thought. Second, salt is modeled as a viscoplastic material, which combines elements of viscous flow and unrecoverable plastic strain. The salt is assumed to be homogeneous halite with isotropic stress, which does not take into account the effects of impurities or the rheological contrasts of other evaporites and non-evaporites in layered evaporite sequences. Furthermore, others have noted that geomechanical models often neglect the importance of water-activated grain-boundary processes and have argued that salt in nature behaves more as a power-law fluid (e.g., Urai et al., 2008).

A related aspect is that stress concentrations do not necessarily result in strain: a given amount of stress will lead to strain in rocks that are weak enough but not in something stronger. Numerical models have been used to model near-salt stress with the goal of predicting associated borehole instability and fracture gradients (e.g., Fredrich et al., 2003, 2007; Willson and Fredrich, 2005; Koupriantchik et al., 2005; Sanz and Dasari, 2010; Nikolinakou et al., 2014, 2018a; 2019; Heidari et al., 2019). The modeled stresses are generally assumed to result in strain, but this may be suspect for two reasons. First, again, the surrounding sediments are treated as weak, cohesionless materials with no shear strength, whereas real minibasin strata are likely strong enough to remain undeformed in most cases. Second, the 'evidence' often cited in support of these models is actually interpretation, for example that folded strata near diapirs or subsalt rubble zones are caused by shear/drag (e.g., Harrison and Patton, 1995; Alsop et al., 2000; Harrison et al., 2004), which we have shown not to be the case.

Whatever the explanation for the mismatch between models and empirical data, the ramifications are important and there are several possible responses. The first is to trust the models and, for example, "fundamentally challenge" (Hamilton-Wright et al., 2019) views that faulting and fracturing are relatively rare around passive diapirs. We argue very much the opposite, namely that observations should be used to ground-truth and test model results. Field work is an absolutely critical component of understanding near-salt deformation, and models need to be refined to match real-world data more closely if they are to be truly useful. Moreover, different types of diapirs must be differentiated – for example, whereas pure passive diapirs are characterized by little small-scale deformation, extensional reactive diapirs are likely to have much more common faulting and fracturing of adjacent strata (as modeled by Hamilton-Wright et al., 2019).

6. Conclusions

This review paper has examined deformation adjacent to passive salt stocks and walls and beneath salt sheets. The existing literature offers a wide variety of models and interpretations, many with diametrically opposed views. On the one hand, some invoke broad zones of intense shear and fracturing caused by salt rise or lateral emplacement; on the other hand, some argue that shear and fracturing are largely absent.

We use primarily outcrop observations to argue here that the latter view is more accurate. In the vast majority of cases, we see no diapir-flanking or subsalt shear (or 'drag') and small-scale fractures are minor. This is not to say that there is no deformation – not at all. Near-diapir deformation is usually present, but most of it falls into two broad categories. The first includes deformation generated by regional tectonics or large-scale minibasin development. The commensurate folds and associated small-scale structures are found throughout the area and typically do not increase in magnitude or intensity above background levels as the salt is approached. There can be exceptions, for example locally concentrated strain caused by squeezing a preexisting stock during regional orogenesis or gravitational failure.

The second category of near-diapir deformation is related to salt flow itself. As we have summarized, this usually causes drape folding of the roof as diapirs rise or sheets advance relative to the flanking minibasins. The folding, in turn, normally leads to the development of faults and fractures, but no more than is the case with any folding. In other words, it is not the flow of the salt *sensu stricto* that causes small-scale deformation; rather, salt rise/emplacement induces folding that in turn causes local faulting and fracturing. In any case, structures indicative of diapir-parallel shear along the salt-sediment interface and within flanking or subsalt strata are practically nonexistent. The vast majority of shear-related structures are those that accommodate flexural-slip during folding. There may in exceptional cases be very narrow zones of shear, especially if the ‘salt’ is relatively strong (stringers or gypsum/anhydrite) and the surrounding strata are anomalously weak. If present, however, they do not extend even meters, let alone hundreds of meters, into the flanking or subsalt strata. Also, there may be damage zones that formed along faults away from the salt that later become juxtaposed against the salt due to ongoing slip.

The observations summarized here have important implications. First, exceptions to the norm are probably evidence of other processes or unusual situations. For example, there may have been local hydraulic fracturing, or very high pore pressures may have weakened the flanking sediments enough to have led to some minor deformation as the salt rose or advanced. Second, those drilling next to diapirs or beneath salt should be aware of the likelihood of typical features such as upturned and even overturned beds, local unconformities, and zones of reworked roof strata. They should be prepared for atypical scenarios of more strained rock that could lead to drilling problems. But they should not expect such situations to be the norm – there are simply too many exposed examples with minimal or no near-diapir deformation (excepting soft-sediment deformation), and most of what is considered to be drag or rubble zones are actually bodies of depositionally reworked roof strata. Finally, it is important to understand the regional setting and the origin and evolution of the diapir or salt sheet. Did it, for example, experience extension or contraction, in which case local faulting and other complications should be anticipated? Or was it simply growing passively, driven by minibasin subsidence, where only drape folding and associated small-scale deformation are to be expected? A solid appreciation of the setting and history can guide those trying to understand what is observed or likely next to stocks/walls and beneath sheets.

Acknowledgements

We thank first the various companies that have sponsored our research over the years, both the Salt-Sediment Interaction Research Consortium at the University of Texas at El Paso (originally at New Mexico State University) and the GeoModels Research Institute at the University of Barcelona. The GeoModels group was partially funded by the SALCOBELT Project (CGL2017-85532-P AEI/FEDER, UE). Without mentioning specific names, we also appreciate the countless conversations we've had in the field with members of the sponsoring companies and different academic institutions. I. Alsop, J. Aschoff, F. Escosa, E. Gannaway Dalton, R. Joussiaume, T. Lawton, M. Nikolinakou, J.-C. Ringenbach, A. Tvedt, and S. Wilkins kindly provided either original figures from their papers or photos that we have included here. Finally, we acknowledge T. Horscroft and the editors of the Journal of Structural Geology for the invitation to contribute this review to the journal, and reviewers XX and YY for helpful comments.

References

Adam, J., Krezsek, C., 2012. Basin-scale salt tectonic processes of the Laurentian Basin, eastern Canada: insights from integrated regional 2D seismic interpretation and 4D physical experiments. In: Alsop, G.I., Archer, S.G., Hartley, A.J., Grant, N.T., Hodgkinson, R. (Eds.), Salt Tectonics, Sediments and Prospectivity. Geol. Soc. Spec. Pub. 363, 331-360. doi:10.1144/SP363.15.

Albertz, M., Beaumont, C., Shimeld, J.W., Ings, S.J., 2010. An investigation of salt tectonic structural styles in the Scotian Basin, offshore Atlantic Canada. Tectonics 29, TC4017. doi:10.1029/2009TC002539.

Albertz, M., Ings, S.J., 2012. Some consequences of mechanical stratification in basin-scale numerical models of passive-margin salt tectonics. In: Alsop, G.I., Archer, S.G., Hartley, A.J., Grant, N.T., Hodgkinson, R. (Eds.), Salt Tectonics, Sediments and Prospectivity. Geol. Soc. Spec. Pub. 363, 303-330. doi:10.1144/SP363.14.

Alsop, G.I., 1996. Physical modelling of fold and fracture geometries associated with salt diapirism. In: Alsop, G.I., Blundell, D.J., Davison, I. (Eds.), Salt Tectonics. Geol. Soc. Spec. Pub. 100, 227-241. doi:10.1144/GSL.SP.1996.100.01.14.

Alsop, G.I., Brown, J.P., Davison, I., Gibling, M.R., 2000. The geometry of drag zones adjacent to salt diapirs. J. Geol. Soc., London 157, 1019-1029. doi:10.1144/jgs.157.5.1019.

Alsop, G.I., Jenkins, G., Davison, I., 1995. A preliminary study of drag zone geometry adjacent to salt diapirs. In: Travis, C.J., Harrison, H., Hudec, M.R., Vendeville, B.C., Peel, F.J., Perkins, B.F. (Eds.), Salt, Sediment, and Hydrocarbons. 16th Annual GCSSEPM Foundation Bob F. Perkins Res. Conf., 1-9. doi:10.5724/gcs.95.16.0001.

Alsop, G.I., Weinberger, R., Levi, T., Marco, S., 2016. Cycles of passive versus active diapirism recorded along an exposed salt wall. J. Struct. Geol. 84, 47-67. doi:10.1016/j.jsg.2016.01.008.

Alsop, G.I., Weinberger, R., Marco, S., Levi, T., 2018. Fault and fracture patterns around a strike-slip influenced salt wall. J. Struct. Geol. 106, 103-124. doi:10.1016/j.jsg.2017.10.010.

Anderson, R., Graham, C.M., Boyce, A.J., Fallick, A.E., 2004. Metamorphic and basin fluids in quartz-carbonate-sulphide veins in the SW Scottish Highlands: a stable isotope and fluid inclusion study. Geofluids 4, 169-185. Doi:10.1111/j.1468-8115.2004.00080.x.

Andrie, J.R., Giles, K.A., Lawton, T.F., Rowan, M.G., 2012. Halokinetic-sequence stratigraphy, fluvial sedimentology and structural geometry of the Eocene Carroza Formation along La Popa salt weld, La Popa

Basin, Mexico. In: Alsop, G.I., Archer, S.G., Hartley, A.J., Grant, N.T., Hodgkinson, R. (Eds.), Salt Tectonics, Sediments and Prospectivity. Geol. Soc. Spec. Pub. 363, 59-79. doi:10.1144/SP363.4.
Aschoff, J.L., Giles, K.A., 2005. Salt diapir-influenced, shallow-marine sediment dispersal patterns: insights from outcrop analogs. AAPG Bull. 89, 447-469. doi:10.1306/10260404016.
Asl, M.E., Faghih, A., Mukherjee, S., Soleimany, B., 2019. Style and timing of salt movement in the Persian Gulf basin, offshore Iran: insights from halokinetic sequences adjacent to the Tonb-e-Bozorg salt diapir. J. Struct. Geol. 122, 116-132. doi:10.1016/j.jsg.2019.02.002.
Baldschuhn, R., Best, G., Kockel, F., 1991. Inversion tectonics in the north-west German basin. In Spencer, A.M. (Ed.), Generation, Accumulation, and Production of Europe's Hydrocarbons. EAPG Spec. Pub. 1, 149-159.
Behrmann, R.B., 1949. Geologie und Lagerstatte des Oelfeldes Reitbruck bei Hamburg. In: Bentz, A. (Ed.), Erdoel und Tektonik in Nordwestdeutschland. Sammelband, Hannover, 190-221.
Bornhauser, M., 1969. Geology of Day dome (Madison County, Texas) – a study of salt emplacement. AAPG Bull. 53, 1411-1420. doi:10.1306/5D25C85B-16C1-11D7-8645000102C1865D.
Brinkmann, R., Lötgers, H., 1968. Diapirs in western Pyrenees and foreland, Spain. In: Braunstein, J., O'Brien, G.D. (Eds.), Diapirs and Diapirism. AAPG Mem. 8, 244-260. doi:10.1306/M8361C18.
Callot, J.-P., Jahani, S., Letouzey, J., 2007. The role of pre-existing diapirs in fold and thrust best development. In: Lacombe, O., Roure, F., Lavé, J., Vergés, J. (Eds.), Thrust Belts and Foreland Basins. Springer, Berlin, 309-325. doi:10.1007-978-3-540-69426-7_16.
Callot, J.-P., Ribes, C., Kergaravat, C., Bonnel, C., Temiz, H., Poisson, A., Vrielynck, B., Salel, J.-F., Ringenbach, J.-C., 2014. Salt tectonics in the Sivas Basin (Turkey): crossing salt walls and minibasins. Bull. Soc. Géol. Fr. 185, 33-42. doi:10.2113/gssgfbull.185.1.33.
Callot, J.-P., Salel, J.-F., Letouzey, J., Daniel, J.-M., Ringenbach, J.-C., 2016. Three-dimensional evolution of salt-controlled minibasins: interactions, folding, and megaflap development. AAPG Bull. 100, 1419-1442. doi:10.1306/03101614087.
Callot, J.-P., Trocmé, V., Letouzey, J., Albouy, E., Jahani, S., Sherkati, S., 2012. Pre-existing salt structures and the folding of the Zagros Mountains. In: Alsop, G.I., Archer, S.G., Hartley, A.J., Grant, N.T., Hodgkinson, R. (Eds.), Salt Tectonics, Sediments and Prospectivity. Geol. Soc. Spec. Pub. 363, 545-561. doi:10.1144/SP363.27.
Canova, D.P., 2017. Comparing the paleohydrologic structure on either side of Witchelina diapir, South Australia. M.S. thesis, Northern Illinois University.
Carruthers, D., Cartwright, J., Jackson, M.P.A., Schutjens, P., 2013. Origin and timing of layer-bound radial faulting around North Sea salt stocks: new insights into the evolving stress state around rising diapirs. Mar. Pet. Geol. 48, 130-148. doi:10.1016/j.marpetgeo.2013.08.001.
Cao, S., Lerche, I., O'Brien, J., 1989. Impact on hydrocarbon retention of sedimentary fracturing and faulting around salt sheets in the Gulf Coast. Gulf Coast Assoc. Geol. Soc. Trans. 39, 15-26.
Choffat, P., 1882. Note préliminaire sur les vallées tiphonique et les éruptions d'ophite et de teschenite en Portugal. Bull. Soc. Géol. Fr. s. 3, 10, 267-288.
Coleman, A.J., Jackson, C.A.-L., Duffy, O.B., Nikolinakou, M.A., 2018. How, where, and when to radial faults grow near salt diapirs? Geol. 46, 655-658. doi:10.1130/G40338.1.
Collon, P., Pichat, A., Kergaravat, C., Botella, A., Caumon, G., Ringenbach, J.-C., Callot, J.-P., 2016. 3D modeling from outcrop data in a salt tectonic context: example from the Inceyol minibasin, Sivas Basin, Turkey. Interpretation 4, SM17-SM31. doi:10.1190/INT-2015-0178.1.
Contreras V., H., Castillón B., M., 1968. Morphology and origin of salt domes in the Isthmus of Tehuantepec. In: Braunstein, J., O'Brien, G.D. (Eds.), Diapirs and Diapirism. AAPG Mem. 8, 244-260. doi:10.1306/M8361C15.
Cross, G.E., 2012. Evaporite deformation in the Sierra Madre Oriental, northeastern Mexico: décollement kinematics in an evaporite-detached thin-skinned fold belt. Ph.D. dissertation, The University of Texas at Austin.
Dalgarno, C.R., Johnson, J.E., 1968. Diapiric structures and Late Precambrian-Early Cambrian sedimentation in Flinders Ranges, South Australia. In: Braunstein, J., O'Brien, G.D. (Eds.), Diapirs and Diapirism. AAPG Mem. 8, 301-314. doi:10.1306/M8361C20.

Daudré, B., Cloetingh, S., 1994. Numerical modelling of salt diapirism: influence of the tectonic regime. Tectonophysics 240, 59-79. doi:10.1016/0040-1951(94)90259-3.
Davies, R.K., Bradbury, W., Fletcher, R., Gavin, L., Welch, M., Knipe, R., 2010. Outcrop observations and analytical models of deformation styles and controls at salt-sediment margins (abs. #90104). AAPG Annual Convention and Exhibition, New Orleans.
Davison, I., Alsop, I., Birch, P., Elders, C., Evans, N., Nicholson, H., Rorison, P., Wade, D., Woodward, J., Young, M., 2000a. Geometry and late-stage structural evolution of Central Graben salt diapirs, North Sea. Mar. Pet. Geol. 17, 499-522. doi:10.1016/S0264-8172(99)00068-9.
Davison, I., Alsop, G.I., Evans, N.G., Safaricz, M., 2000b. Overburden deformation patterns and mechanisms of salt diapir penetration in the Central Graben, North Sea. Mar. Pet. Geol. 17, 601-618. doi:10.1016/S0264-8172(00)00011-8.
Davison, I., Barreto, P., 2019. Salt tectonics and hydrocarbon accumulations trapped on diapir flanks in the Lusitanian Basin, Portugal. In: Fiduk, J.C., Mount, V., Hearon, T.E. IV (Eds.), Salt Tectonics, Associated Processes, and Exploration Potential: Revisited 1989-2019. GCSSEPM Foundation Perkins-Rosen Research Conference, 300-313.
Davison, I., Bosence, D., Alsop, I., Al-Aawah, M.H., 1995. Deformation and sedimentation above and below Miocene salt diapirs and their overhangs, NW Yemen. In: Travis, C.J., Harrison, H., Hudec, M.R., Vendeville, B.C., Peel, F.J., Perkins, B.F. (Eds.), Salt, Sediment, and Hydrocarbons. 16th Annual GCSSEPM Foundation Bob F. Perkins Res. Conf., 33-40. doi:10.5724/gcs.95.16.0033.
Davison, I., Bosence, D., Alsop, G.I., Al-Aawah, M.H., 1996. Deformation and sedimentation around active Miocene salt diapirs on the Tihama Plain, northwest Yemen. In: Alsop, G.I., Blundell, D.J., Davison, I. (Eds.), Salt Tectonics. Geol. Soc. Spec. Pub. 100, 23-39. doi:10.1144/GSL.SP.1996.100.01.03.
Davison, I., Insley, M. Harper, M., Weston, P., Blundell, D., McClay, K., Qualington, A., 1993. Physical modelling of overburden deformation around salt diapirs. Tectonophysics 228, 255-274. doi:10.1016/0040-1951(93)90344-J.
Diegel, F.A., Karlo, J.F., Schuster, D.C., Shoup, R.C., Tauvers, P.R., 1995. Cenozoic structural evolution and tectono-stratigraphic framework of the northern Gulf Coast continental margin. In: Jackson, M.P.A., Roberts, D.G., Snelson, S. (Eds.), Salt Tectonics: a Global Perspective. AAPG Mem. 65, 109-151. doi:10.1306/M65604C6.
Dixon, J.M., 1975. Finite strain and progressive deformation in models of diapiric structures. Tectonophysics 28, 89-124. doi:10.1016/0040-1951(75)90060-8.
Dooley, T.B., Hudec, M.R., Jackson, M.P.A., 2012. The structure and evolution of sutures in allochthonous salt. AAPG Bull. 96, 1045-1070. doi:10.1306/09231111036.
Dooley, T.B., Jackson, M.P.A., Hudec, M.R., 2014. Breakout of squeezed stocks: dispersal of roof fragments, source of extrusive salt and interaction with regional thrust faults. Bas. Res. 26, 3-25. doi:10.1111/bre.12056.
Dooley, T., McClay, K., Hempton, M., Smit, D., 2005. Salt tectonics above complex basement extensional fault systems: results from analogue modelling. In Doré, A.G., Vining, B.A. (Eds.), Petroleum Geology: North-West Europe and Global Perspectives – Proceedings of the 6th Petroleum Geology Conference. Geological Society, London, 1631-1648. doi:10.1144/0061631.
Duffy, O.B., Dooley, T.P., Hudec, M.R., Jackson, M.P.A., Fernandez, N., Jackson, C.A.-L., Soto, J.I., 2018. Structural evolution of salt-influenced fold-and-thrust belts: a synthesis and new insights from basins containing isolated salt diapirs. J. Struct. Geol. 114, 206-221. doi:10.1016/j.jsg.2018.06.024.
Escosa, F.O., Rowan, M.G., Giles, K.A., Deatrick, K.T., Mast, A.M., Langford, R.P., Hearon, T.E. IV, Roca, E., 2018. Lateral terminations of salt walls and megaflaps: an example from Gypsum Valley diapir, Paradox Basin, Colorado, USA. Bas. Res. 31, 191-212. doi:10.1111/bre.12316.
Eskozha, B.A., 2008. Structural features and petroleum potential of the Triassic series of the eastern Precaspian basin. Izvestiya NAN RK, Seriya Geologicheskaya 4, 38-48.

Evans, M.A., Battles, D.A., 1999. Fluid inclusion and stable isotope analyses of veins from the central Appalachian Valley and Ridge province: implications for regional synorogenic hydrologic structure and fluid migration. GSA Bull. 111, 1841-1860. doi:10.1130/0016-7606(1999)111%3C1841:FIASIA%3E2.3.CO;2.

Ferrer, O., Roca, E., Muñoz, J.A., Rowan, M.G., Carrera, N., Giles, K.A., 2018. Kinematic evolution of halokinetic and contractional megaflaps: insights from analog modelling and application to case studies. GeoMod 2018, Barcelona.

Fiduk, J.C., Clippard, M., Power, S., Robertson, V., Rodriguez, L., Ajose, O., Fernandez, D., Smith, D., 2014. Origin, transportation, and deformation of Mesozoic carbonate rafts in the northern Gulf of Mexico. GCAGS J. 3, 20-32.

Fiduk, J.C., Robertson, V., Clippard, M., Jamieson, G.A., Power, S., 2016. Extensional salt keels detached on Eocene-Oligocene sediments in the deepwater northern Gulf of Mexico: insights into canopy advancement, salt-sediment interplay, and evidence for unrecognized mass sediment displacement. GCAGS J. 5, 47-63.

Fischer, M.P., Jackson, P.B., 1999. Stratigraphic controls on deformation patterns in fault-related folds: a detachment fold example from the Sierra Madre Oriental, northeast Mexico. J. Struct. Geol. 21, 613-633. doi:10.1016/S0191-8141(99)00044-9.

Fredrich, J.T., Coblenz, D., Fossum, A.F., Thorne, B.J., 2003. Stress perturbations adjacent to salt bodies in the deepwater Gulf of Mexico. Soc. Pet. Eng. SPE 84554. SPE Annual Technical Conference and Exhibition, Denver. doi:10.2118/84554-MS.

Fredrich, J.T., Engler, B.P., Smith, J.A., Onyia, E.C., Tolman, D.N., 2007. Predrill estimation of subsalt fracture gradient: analysis of the Spa prospect to validate nonlinear finite element stress analyses. Soc. Pet. Eng. SPE/IADC 105763. SPE/IADC Drilling Conference, Amsterdam. doi:10.2118/105763-MS.

Gannaway Dalton, C.E., Giles, K.A., Muñoz, J.A., Rowan, M.G., 2020a. Sedimentologic and sequence-stratigraphic characterization of salt-related basins and megaflaps at the Aulet and Adons diapirs, Spanish Pyrenees, Catalunya. Mar. Pet. Geol., in review.

Gannaway Dalton, C.E., Giles, K.A., Rowan, M.G., Langford, R.P., Hearon, T.E. IV, Fiduk, J.C., 2020b. Sedimentologic, stratigraphic, and structural evolution of minibasins and a megaflap formed during passive salt diapirism: the Neoproterozoic Witchelina diapir, Willouran Ranges, South Australia. J. Sed. Res. 90, 165-199. doi:10.2110/jsr.2020.9.

Ge, H., Jackson, M.P.A., Vendeville, B.C., 1997. Kinematics and dynamics of salt tectonics driven by progradation. AAPG Bull. 81, 398-423. doi:10.1306/522B4361-1727-11D7-8645000102C1865D.

Ge, H., Jackson, M.P.A., 1998. Physical modeling of structures formed by salt withdrawal: implications for deformation caused by salt dissolution. AAPG Bull. 82, 228-250. doi:10.1306/1D9BC3DB-172D-11D7-8645000102C1865D.

Gemmer, L., Beaumont, C., Ings, S.J., 2005. Dynamic modelling of passive margin salt tectonics: effects of water loading, sediment properties and sedimentation patters. Bas. Res. 17, 383-402. doi:10.1111/j.1365-2117.2005.00274.x.

Giles, K.A., Druke, D.C., Mercer, D.W., Hunnicutt-Mack, L., 2008. Controls on Upper Cretaceous (Maastrichtian) heterozoan carbonate platforms developed on salt diapirs, La Popa Basin, NE Mexico. In: Lukasik, J., Simo, J.A. (Eds.), Controls on Carbonate Platform and Reef Development. SEPM Spec. Pub. 89, 107-124. doi:10.2110/pec.08.89.0107.

Giles, K.A., Lawton, T.F., 2002. Halokinetic sequence stratigraphy adjacent to the El Papalote diapir, northeastern Mexico. AAPG Bull. 86, 823-840. doi:10.1306/61EEDBAC-173E-11D7-8645000102C1865D.

Giles, K.A., Rowan, M.G., 2012. Concepts in halokinetic-sequence deformation and stratigraphy. In: Alsop, G.I., Archer, S.G., Hartley, A.J., Grant, N.T., Hodgkinson, R. (Eds.), Salt Tectonics, Sediments and Prospectivity. Geol. Soc. Spec. Pub. 363, 7-31. doi:10.1144/SP363.2.

Giles, K.A., Rowan, M.G., Langford, R., McFarland, J., Hearon, T., 2018. Salt shoulders. AAPG Search and Discovery #30554.

Gradmann, S., Beaumont, C., 2016. Numerical modelling study of mechanisms of mid-basin salt canopy evolution and their potential applications to the northwestern Gulf of Mexico. Bas. Res. 29, 490-520. doi:10.1111/bre.12186.

Graham, R., Jackson, M.P.A., Pilcher, R., Kilsdonk, B., 2012. Allochthonous salt in the sub-Alpine fold-thrust belt of Haute Provence, France. In: Alsop, G.I., Archer, S.G., Hartley, A.J., Grant, N.T., Hodgkinson, R. (Eds.), Salt Tectonics, Sediments and Prospectivity. Geol. Soc. Spec. Pub. 363, 595-615. doi:10.1144/SP363.30.

Hamilton-Wright, J., Dee, S., von Nicolai, C., Johnson, H., 2019. Investigating controls on salt movement in extensional settings using finite-element modelling. Pet. Geosci. 25, 258-271. doi:10.1144/petgeo2018-119.

Handschy, J., van den Beukel, J., Ge, H., Diegel, F., 1998. Salt-dome geometries, Gulf of Mexico shelf (abs.) AAPG Annual Convention and Exhibition, Salt Lake City.

Hanna, M.A., 1953. Fracture porosity in Gulf Coast. AAPG Bull. 37, 266-281. doi:10.1306/5CEADC53-16BB-11D7-8645000102C1865D.

Harding, R., Huuse, M., 2015. Salt on the move: multi-stage evolution of salt diapirs in the Netherlands North Sea. Mar. Pet. Geol. 61, 39-55. doi:10.1016/j.marpetgeo.2014.12.003.

Harrison, H., Kuhmichel, L., Heppard, P., Milkov, A.V., Turner, J.C., Greeley, D., 2004. Base of salt structure and stratigraphy – data and models from Pompano field, VK 989/990, Gulf of Mexico. In: Post, P.J., Olson, D.L., Lyons, K.T., Palmes, S.L., Harrison, P.F., Rosen, N.C. (Eds.), Salt-Sediment Interactions and Hydrocarbon Prospectivity: Concepts, Applications, and Case Studies for the 21st Century. 24th Annual GCSSEPM Foundation Bob F. Perkins Research Conference, 243-269. doi:10.5724/gcs.04.24.0243.

Harrison, H.L, Patton, B., 1995. Translation of salt sheets by basal shear. In: Travis, C.J., Harrison, H., Hudec, M.R., Vendeville, B.C., Peel, F.J., Perkins, B.F. (Eds.), Salt, Sediment, and Hydrocarbons: 16th Annual GCSSEPM Foundation Bob F. Perkins Res. Conf., 99-107. doi:10.5724/gcs.95.16.0099.

Harrison, J.C., Jackson, M.P.A., 2014. Exposed evaporite diapirs and minibasins above a canopy in central Sverdrup Basin, Axel Heiberg Island, Arctic Canada. Bas. Res. 26, 567-596. doi:10.1111/bre.12037.

Hearon, T.E. IV, Rowan, M.G., Giles, Hart, W.H., 2014. Halokinetic deformation adjacent to the deepwater Auger diapir, Garden Banks 470, northern Gulf of Mexico: testing the applicability of an outcrop-based model using subsurface data. Interpretation 2, SM57-SM76. doi:10.1190/INT-2014-0053.1.

Hearon, T.E. IV, Rowan, M.G., Giles, K.A., Kernen, R.A., Gannaway, C.E., Lawton, T.F., Fiduk, J.C., 2015a. Allochthonous salt initiation and advance in the northern Flinders and eastern Willouran Ranges, South Australia: using outcrops to test subsurface-based models from the northern Gulf of Mexico. AAPG Bull. 99, 293-331. doi:10.1306/08111414022.

Hearon, T.E. IV, Rowan, M.G., Lawton, T.F., Hannah, P.T., Giles, K.A., 2015b. Geology and tectonics of Neoproterozoic salt diapirs and salt sheets in the eastern Willouran Ranges, South Australia. Bas. Res. 27, 183-207. doi:10.1111/bre.12067.

Heidari, M., Nikolinakou, M.A., Flemings, P.B., Hudec, M.R., 2017. A simplified stress analysis of rising salt domes. Bas. Res. 29, 363-376. doi:10.1111/bre.12181.

Heidari, M., Nikolinakou, M.A., Hudec, M.R., Flemings, P.B., 2016. Geomechanical analysis of a welding salt layer and its effects on adjacent sediments. Tectonophysics 683, 172-181. doi:10.1016/j.tecto.2016.06.027.

Heidari, M., Nikolinakou, M.A., Hudec, M.R., Flemings, P.B., 2019. Influence of a reservoir bed on diapirism and drilling hazards near a salt diapir: a geomechanical approach. Pet. Geosci. 25, 282-297. doi:10.1144/petgeo2018-113.

Hempel, P.M., 1967. Der Diapir von Poza de la Sal (Nordspanien). Bei. Geol. Jahrbuch 66, 95-126.

Hennessy, B.E., 2009. Characterization of syn-depositional faulting of a composite wedge halokinetic sequence along the La Popa salt weld, La Popa Basin, Nuevo Leon, Mexico. M.S. thesis, New Mexico State University.

House, W.M., Pritchett, J.A., 1995. Fluid migration and formation pressures associated with allochthonous salt sheets in the northern Gulf of Mexico. In: Travis, C.J., Harrison, H., Hudec, M.R., Vendeville, B.C., Peel, F.J., Perkins, B.F. (Eds.), Salt, Sediment, and Hydrocarbons. 16th Annual GCSSEPM Foundation Bob F. Perkins Res. Conf., 121-124. doi:10.5724/gcs.95.16.0121.

Hudec, M.R., Jackson, M.P.A., 2006. Advance of allochthonous salt sheets in passive margins and orogens. AAPG Bull. 90, 1535-1564. doi:10.1306/05080605143.

Hudec, M.R., Jackson, M.P.A., 2009. Interaction between spreading salt canopies and their peripheral thrust systems. J. Struct. Geol. 31, 1114-1129. doi:10.1016/j.jsg.2009.06.005.

Hudec, M.R., Jackson, M.P.A., 2011. The Salt Mine – a Digital Atlas of Salt Tectonics. Udden Book Series No. 5, AAPG Mem. 99. Bur. Econ. Geol., Austin.

Hudec, M.R., Jackson, M.P.A., Schultz-Ela, D.D., 2009. The paradox of minibasin subsidence into salt: clues to the evolution of crustal basins. GSA Bull. 121, 201-221. doi:10.1130/B26275.1.

Ings, S.J., Shimeld, J.W., 2006. A new conceptual model for the structural evolution of a regional salt detachment on the northeast Scotian margin, offshore eastern Canada. AAPG Bull. 90, 1407-1423. doi:10.1306/04050605159.

Jackson, M.P.A., 1995. Retrospective salt tectonics. In: Jackson, M.P.A., Roberts, D.G., Snelson, S. (Eds.), Salt Tectonics: a Global Perspective. AAPG Mem. 65, 1-28. doi:10.1306/M65604.

Jackson, M.P.A., Cornelius, R.R., 1987. Stepwise centrifuge modeling of the effects of differential sediment loading on the deformation of salt structures. In: Lerche, I., O'Brien, J.J. (Eds.), Dynamical Geology of Salt and Related Structures. Academic Press, Orlando.

Jackson, M.P.A., Cornelius, R.R., Craig, C.H., Gansser, A., Stöcklin, J., Talbot, C.J., 1990. Salt Diapirs of the Great Kavir, Central Iran. GSA Mem. 177. doi:10.1130/MEM177.

Jackson, M.P.A., Hudec, M.R., 2004. A new mechanism for advance of allochthonous salt sheets. In: Post, P.J., Olson, D.L., Lyons, K.T., Palmes, S.L., Harrison, P.F., Rosen, N.C. (Eds.), Salt-Sediment Interactions and Hydrocarbon Prospectivity: Concepts, Applications, and Case Studies for the 21st Century. 24th Annual GCSSEPM Foundation Bob F. Perkins Research Conference, 220-242. doi:10.5724/gcs.04.24.0220.

Jackson, M.P.A., Hudec, M.R., 2017. Salt Tectonics – Principles and Practice. Cambridge Univ. Press, Cambridge.

Jackson, M.P.A., Schultz-Ela, D.D., Hudec, M.R., Watson, I.A., Porter, M.L., 1998. Structure and evolution of Upheaval Dome: a pinched-off salt diapir. GSA Bull. 110, 1547-1573. doi:10.1130/0016-7606(1998)110%3C1547:SAEOUD%3E2.3.CO;2.

Jackson, M.P.A., Talbot, C.J., 1991. A Glossary of Salt Tectonics. Geological Circular 91-4. Bur. Econ. Geol., Austin. doi:10.23867/gc9104D.

Jackson, M.P.A., Talbot, C.J., Cornelius, R.R., 1988, Centrifuge Modeling of the Effects of Aggradation and Progradation on Syndepositional Salt Structures. Report of Investigations 173. Bur. Econ. Geol., Austin.

Jahani, S., Callot, J.-P., Letouzey, J., Frizon de Lamotte, D., 2009. The eastern termination of the Zagros Fold-and-Thrust Belt, Iran: structures, evolution, and relationships between salt plugs, folding, and faulting. Tectonics 28, TC6004. doi:10.1029/2008TC002418.

Johnson, H.A., Bredeson, D.H., 1971. Structural development of some shallow salt domes in Louisiana Miocene productive belt. AAPG Bull. 55, 204-226. doi:10.1306/5D25CE19-16C1-11D7-8645000102C1865D.

Karam, P., Mitra, S., 2016. Experimental studies of the controls of the geometry and evolution of salt diapirs. Mar. Pet. Geol. 77, 1309-1322. doi:10.1016/j.marpetgeo.2016.05.010.

Kergaravat, C., 2016. Dynamique de formation et de déformation de mini-bassins en contexte compressif: exemple du bassin de Sivas, Turquie. Ph.D. dissertation, Université de Pau et des Pays de l'Adour.

Kergaravat, C., Ribes, C., Callot, J.-P., Ringenbach, J.-C., 2017. Tectono-stratigraphic evolution of salt-controlled minibasins in a fold-and-thrust belt, the Oligo-Miocene central Sivas Basin. J. Struct. Geol. 102, 75-97. doi:10.1016/j.jsg.2017.07.007.

Kergaravat, C., Ribes, C., Legeay, E., Callot, J.-P., Kavak, K.S., Ringenbach, J.-C., 2016. Minibasins and salt canopy in foreland fold-and-thrust belts: the central Sivas Basin, Turkey. Tectonics 35. doi:10.1002/2016TC004186.

Kernen, R.A., Giles, K.A., Rowan, M.G., Lawton, T.F., Hearon, T.E. IV, 2012. Depositional and halokinetic-sequence stratigraphy of the Neoproterozoic Wonoka Formation adjacent to Patawarta allochthonous salt sheet, Central Flinders Ranges, South Australia. In: Alsop, G.I., Archer, S.G., Hartley, A.J., Grant, N.T., Hodgkinson, R. (Eds.), Salt Tectonics, Sediments and Prospectivity. Geol. Soc. Spec. Pub. 363, 81-105. doi:10.1144/SP363.5.

Kerr, P.F., Kopp, O.C., 1958. Salt-dome breccia. AAPG Bull. 42, 548-560. doi:10.1306/0BDA5AA4-16BD-11D7-8645000102C1865D.

Kilby, R.W., Diegel, F.A., Styzen, M.J., 2008. Age of sediments encasing allochthonous salt in the Gulf of Mexico: clues to emplacement history (abs.) AAPG Annual Convention, San Antonio.

Kolarsky, R.A., 1996. Interaction between salt diapir growth and sedimentation: an example from Côte Blanche Island field, Louisiana (abs.). Gulf Coast Assoc. Geol. Soc. Trans. 61, 655.

Koupriantchik, D., Hunt, S.P., Meyers, A.G., 2005. Geomechanical modeling of salt diapirs: a field-scale analysis for a 3D salt structure from the North Sea. ISRM International Symposium – EUROCK 2005, Brno.

Koyi, H., 1996. Salt flow by aggrading and prograding overburdens. In: Alsop, G.I., Blundell, D.J., Davison, I. (Eds.), Salt Tectonics. Geol. Soc. Spec. Pub. 100, 243-258. doi:10.1144/GSL.SP.1996.100.01.15.

Koyi, H., Talbot, C.J., Tørudbakken, B.O., 1993. Salt diapirs of the southwest Nordkapp Basin: analogue modelling. Tectonophysics 228, 167-187. doi:10.1016/0040-.1951(93)90339-L

Krzywiec, P., 2009. Geometria I ewolucja wybranych struktur solnych z obszaru Niżu Polskiego w świetle danych sejsmicznych. Przegląd Geol. 57, 812-818.

Kupfer, D.H., 1968. Relationship of internal to external structure of salt domes. In: Braunstein, J., O'Brien, G.D. (Eds.), Diapirs and Diapirism. AAPG Mem. 8, 79-89. doi:10.1306/M8361C5.

Langford, R.P., Giles, K.A., Bailey, C., Soltero, A., Lankford-Bravo, D., 2020. Salt shoulders of the Paradox Basin. AAPG Bull., in review.

Lankford-Bravo, D., Giles, K.A., Langford, R., 2019. Characterization of syndepositional deformation in the Permian Cutler Formation, northern margin Onion Creek diapir, Paradox Basin, UT (abs.). GSA Annual Meeting, Phoenix. https://gsa.confex.com/gsa/2019AM/meetingapp.cgi/Paper/333541

Lawton, T.F., Buck, B.J., 2006. Implications of diapir-derived detritus and gypsic paleosols in Lower Triassic strata near the Castle Valley salt wall, Paradox Basin, Utah. Geol. 34, 885-888. doi:10.1130/G22574.1.

Lawton, T.F., Buller, C.D., Parr, T.R., 2015. Provenance of a Permian erg on the western margin of Pangea: depositional system of the Kungurian (late Leonardian) Castle Valley and White Rim sandstones and subjacent Cutler Group, Paradox Basin, Utah, USA. Geosphere 11. doi:10.1130/GES01174.1.

Lemon, N.M., 1985. Physical modeling of sedimentation adjacent to diapirs and comparison with Late Precambrian Oratunga breccia body in Central Flinders Ranges, South Australia. AAPG Bull. 69, 1327-1338. doi:10.1306/AD462C59-16F7-11D7-8645000102C1865D.

Letouzey, J., Sherkati, S., 2004. Salt movement, tectonic events, and structural style in the Central Zagros Fold and Thrust Belt (Iran). In: Post, P.J., Olson, D.L., Lyons, K.T., Palmes, S.L., Harrison, P.F., Rosen, N.C. (Eds.), Salt-Sediment Interactions and Hydrocarbon Prospectivity: Concepts, Applications, and Case Studies for the 21st Century. 24th Annual GCSSEPM Foundation Bob F. Perkins Research Conference, 220-242. doi:10.5724/gcs.04.24.0753.

Li, Z., Fischer, M., 2017. Stress modeling around the toe of an advancing salt sheet (abs.) Workshop on Analog Modeling of Tectonic Processes, Austin.

López-Mir, B., Muñoz, J.A., García-Senz, J., 2014. Extensional salt tectonics in the partially inverted Cotiella post-rift basin (south-central Pyrenees): structure and evolution. Int. J. Earth Sci. doi:10.1007/s00531-014-1091-9.

López-Mir, B., Schneider, S., Hülse, P., 2017. Fault activity and diapirism in the Mississippian to Late Cretaceous Sverdrup Basin: new insights into the tectonic evolution of the Canadian Arctic. J. Geodynam. 118, 55-65. doi:10.1016/j.jog.2017.11.002.

Luo, G., Nikolinakou, M.A., Flemings, P.B., Hudec, M.R., 2012. Geomechanical modeling of stresses adjacent to salt bodies: Part 1 – uncoupled models. AAPG Bull. 94, 43-64. doi:10.1306/04111110144.

Martín-Martín, J.D., Vergés, J., Saura, E., Moragas, M., Messager, G., Baqués, V., Razin, P., Grélaud, C., Malaval, M., Joussiaume, R., Casciello, E., Cruz-Orosa, I., Hunt, D.W., 2016. Tectonics 35. doi:10.1002/2016TC004300.

Mast, A.M., 2016. The origin of anomalous carbonate units outcropping at the salt-sediment interface of the southern end of Gypsum Valley salt wall, Paradox Basin, Colorado. M.S. thesis, The University of Texas at El Paso.

Mattos, N.H., Alves, T.M., 2018. Corridors of crestal and radial faults linking salt diapirs in the Espírito Santo Basin, SE Brazil. Tectonophysics 728-729, 55-74. doi:10.1016/j.tecto.2017.12.025.

Maunde, A., Alves, T.M., 2020. Impact of tectonic rafts' gravitational instability on fault reactivation and geometry. J. Struct. Geol. 130. doi:10.1016/j.jsg.2019.103916.

McFarland, J.C., 2016. Structural and stratigraphic development of a salt-diapir shoulder, Gypsum Valley, Colorado. M.S. thesis, The University of Texas at El Paso.

Mount, V.S., Wilkins, S.J., Lindsey, B., Butaud, T., Gamwell, P., Fowler, T., Morris, C., Adiguna, H., McDonald, B., 2019. Structural configuration and evolution of subsalt hydrocarbon traps adjacent to salt walls, Green Canyon, Gulf of Mexico. In: Fiduk, J.C., Mount, V., Hearon, T.E. IV (Eds.), Salt Tectonics, Associated Processes, and Exploration Potential: Revisited 1989-2019. GCSSEPM Foundation Perkins-Rosen Research Conference, 347-356.

Murray, G.E., 1966. Salt structures of Gulf of Mexico basin – a review. AAPG Bull. 50, 439-478. doi:10.1306/5D25B49D-16C1-11D7-8645000102C1865D.

Murray, G.E., 1968. Salt structures of Gulf of Mexico basin – a review. In: Braunstein, J., O'Brien, G.D. (Eds.), Diapirs and Diapirism. AAPG Mem. 8, 99-121. doi:10.1306/M8361C7.

Nettleton, L.L., 1934. Fluid mechanics of salt domes. AAPG Bull. 18, 1175-1204. doi:10.1306/3D932C74-16B1-11D7-8645000102C1865D.

Nettleton, L.L., 1943. Recent experimental and geophysical evidence of mechanics of salt-dome formation. AAPG Bull. 27, 51-63. doi:10.1306/3D933588-16B1-11D7-8645000102C1865D

Nettleton, L.L., 1955. History of concepts of Gulf Coast salt-dome formation. AAPG Bull. 39, 2373-2383. doi:10.1306/5CEAE2DA-16BB-11D7-8645000102C1865D.

Nettleton, L.L., Elkins, T.A., 1947. Geologic models made from granular materials. AGU Trans. 28, 451-466. doi:10.1029/TR028i003p00451.

Nikolinakou, M.A., Flemings, P.B., Heidari, M., Hudec, M.R., 2018a. Stress and pore pressure in mudrocks bounding salt systems. Rock Mech. Rock Eng. doi:10.1007/s00603-018-1540-z

Nikolinakou, M.A., Flemings, P.B., Hudec, M.R., 2014. Modeling stress evolution around a rising salt diapir. Mar. Pet. Geol. 51, 230-238. doi:10.1016/j.marpetgeo.2013.11.021.

Nikolinakou, M.A., Heidari, M., Flemings, P.G., Hudec, M.R., 2018b. Geomechanical modeling of pore pressure in evolving salt systems. Mar. Pet. Geol. 93, 272-286. doi:10.1016/j.marpetgeo.2018.03.013.

Nikolinakou, M.A., Heidari, M., Hudec, M.R., Flemings, P.B., 2017. Initiation and growth of salt diapirs in tectonically stable settings: upbuilding and megaflaps. AAPG Bull. 101, 887-905. doi:10.1306/09021615245.

Nikolinakou, M.A., Heidari, M., Hudec, M.R., Flemings, P.B., 2019. Stress and deformation in plastic mudrocks overturning in front of advancing salt sheets; implications for system kinematics and drilling. Rock Mech. Rock Eng. doi:10.1007/s00603-019-01852-2.

Nikolinakou, M.A., Luo, G., Hudec, M.R., Flemings, P.B., 2012. Geomechanical modeling of stresses adjacent to salt bodies: Part 2 – poroelasticity and coupled overpressures. AAPG Bull. 94, 65-85. doi:10.1306/04111110144.

Parker, T.J., McDowell, A.N., 1951. Scale models as guide to interpretation of salt-dome faulting. AAPG Bull. 35. 2076-2086. doi:10.1306/3D934322-16B1-11D7-8645000102C1865D.

Parker, T.J., McDowell, A.N., 1955. Model studies of salt-dome tectonics. AAPG Bull. 39, 2384-2470. doi:10.1306/5CEAE2DD-16BB-11D7-8645000102C1865D.

Pichat, A., Hoareau, G., Callot, J.-P., Ringenbach, J.-C., 2019. Characterization of Oligo-Miocene evaporite-rich minibasins in the Sivas Basin, Turkey. Mar. Pet. Geol. 110, 587-605. doi:10.1016/j.marpetgeo.2019.07.050.

Pichel, L.M., Jackson, C.A.-L., 2020. Four-dimensional variability of composite halokinetic sequences. Bas. Res. doi:10.1111/bre.12428.

Podlachikov, Y., Talbot, C., Poliakov, A.N.B., 1993. Numerical models of complex diapirs. Tectonophysics 228, 189-198. doi:10.1016/0040-1951(93)90340-P.

Poprawski, Y., Basile, C., Jaillard, E., Gaudin, M., Lopez, M., 2016. Halokinetic sequences in carbonate systems: an example from the middle-Albian Bakio breccias formation (Basque Country, Spain). Sed. Geol. 334, 34-52. doi:10.1016/j.sedgeo.2016.01.013.

Poprawski, Y., Basile, C., Agirrezabala, L.M., Jaillard, E., Gaudin, M., Jacquin, T., 2014. Sedimentary and structural record of the Albian growth of the Bakio salt diapir (the Basque Country, northern Spain). Bas. Res. 26, 746-766. doi:10.1111/bre.12062.

Pošepný, F., 1871. Studien aus den Salinargebiete Siebenbürgens. Kaiserlich-Königlichen Geologischen Reichanstalt Jahrbuch 21, 123-186.

Quintà, A., Tavani, S., Roca, E., 2012. Fracture pattern analysis as a tool for constraining the interaction between regional and diapir-related stress fields: Poza de la Sal diapir (Basque Pyrenees, Spain). In: Alsop, G.I., Archer, S.G., Hartley, A.J., Grant, N.T., Hodgkinson, R. (Eds.), Salt Tectonics, Sediments and Prospectivity. Geol. Soc. Spec. Pub. 363, 521-532. doi:10.1144/SP363.25.

Ramberg, H., 1981. The role of gravity in orogenic belts. Geol. Soc., London, Spec. Pub. 9, 125-140. doi:10.1144/GSL.SP.1981.009.01.11.

Ringenbach, J.-C., Salel, J.-F., Kergaravat, C., Ribes, C., Bonnel, C., Callot, J.-P., 2013. Salt tectonics in the Sivas Basin, Turkey: outstanding seismic analogues from outcrops. First Break 31, 93-101. doi:10.3997/1365-2397.2013016.

Roca, E., Anadón, P., Utrilla, R., Vázquez, A., 1996. Rise, closure and reactivation of the Bicorb-Quesa evaporite diapir, eastern Prebetics, Spain. J. Geol. Soc., London, 153, 311-321. doi:10.1144/gsjgs.153.2.0311.

Roca, E., Ferrer, O., Rowan, M.G., Muñoz, J.A., Butillé, M., Giles, K.A., Arbués, P., de Matteis, M., 2020. Salt tectonics and salt-sediment interaction at deepwater diapirs: lessons from the outcropping Bakio diapir, Basque-Cantabrian Basin, Pyrenees. Mar. Pet. Geol., in review.

Rojo, L.A., Escalona, A., 2018. Controls on minibasin infill in the Nordkapp basin: evidence of complex Triassic synsedimentary deposition influenced by salt tectonics. AAPG Bull. 102, 1239-1272. doi:10.1306/0926171524316523.

Rojo, L.A., Escalona, A., Schulte, L., 2016. The use of seismic attributes to enhance imaging of salt structures in the Barents Sea. First Break 34, 49-57. doi:10.3997/1365-2397-2016014.

Rowan, M.G., 2017. An overview of allochthonous salt tectonics. In: Soto, J.I., Flinch, J.F., Tari, G. (Eds.), Permo-Triassic salt provinces of Europe, North Africa and the Atlantic margins. Elsevier, Amsterdam, 97-114. doi:10.1016/B978-0-12-809417-4.00005-7.

Rowan, M.G., 2020. Salt- and shale-detached gravity-driven failure of continental margins. In: Scarselli, N., Adam, J., Chiarella, D. (Eds.), Regional Geology and Tectonics: Principles of Geologic Analysis, 2nd Ed. Elsevier, Amsterdam, in press.

Rowan, M.G., Giles, K.A., 2020, Passive vs active salt diapirism. AAPG Bull., in review.

Rowan, M.G., Giles, K.A., Hearon, T.E. IV, Fiduk, J.C., 2016. Megaflaps adjacent to salt diapirs. AAPG Bull. 100, 1723-1747. doi:10.1306/05241616009.

Rowan, M.G., Giles, K.A., Roca, E., Arbués, P., Ferrer, O., 2012a. Analysis of growth strata adjacent to an exposed deepwater salt diapir, northern Spain (abs.). AAPG Annual Convention and Exhibition, Long Beach.

Rowan, M.G., Hearon, T.E. IV, Kernen, R.A., Giles, K.A., Gannaway-Dalton, C.E., Williams, N.J., Fiduk, J.C., Lawton, T.F., Hannah, P.T., Fischer, M.P., 2019a. A review of allochthonous salt tectonics in the Flinders and Willouran ranges, South Australia. Austral. J. Ear. Sci. doi:10.1080/08120099.2018.1553063.

Rowan, M.G., Inman, K.F., 2005. Counterregional-style deformation in the deep shelf of the northern Gulf of Mexico. Gulf Coast Assoc. Geol. Soc. Trans. 55, 716-724.

Rowan, M.G., Lawton, T.F., Giles, K.A., 2012b. Anatomy of an exposed vertical salt weld and flanking strata, La Popa Basin, Mexico. In: Alsop, G.I., Archer, S.G., Hartley, A.J., Grant, N.T., Hodgkinson, R. (Eds.), Salt Tectonics, Sediments and Prospectivity. Geol. Soc. Spec. Pub. 363, 33-57. doi:10.1144/SP363.3.

Rowan, M.G., Lawton, T.F., Giles, K.A., Ratliff, R.A., 2003. Near-salt deformation in La Popa basin, Mexico, and the northern Gulf of Mexico: a general model for passive diapirism. AAPG Bull., 87, 733-756. doi:10.1306/01150302012.

Rowan, M.G., Ratliff, R.A., 2012. Cross-section restoration of salt-related deformation: best practices and potential pitfalls. J. Struct. Geol. 41, 24-37. doi:10.1016/j.jsg.2011.12.012.

Rowan, M.G., Urai, J.L., Fiduk, J.C., Kukla, P.A., 2019b. Deformation of intrasalt competent layers in different modes of salt tectonics. Solid Earth 10, 987-1013. doi:10.5194/se-10-987-2019.

Rowan, M.G., Vendeville, B.C., 2006. Foldbelts with early salt withdrawal and diapirism: physical model and examples from the northern Gulf of Mexico and the Flinders Ranges, Australia. Mar. Pet. Geol. 26, 871-891. doi:10.1016/j.marpetgeo.2006.08.003.

Salazar, J.A., Knapp, J.H., Knapp, C.C., Pyles, D.R., 2014. Salt tectonics and Pliocene stratigraphic framework at MC-118, Gulf of Mexico: an integrated approach with application to deep-water confined structures in salt basins. Mar. Pet. Geol. 50, 51-67. doi:10.1016/j.marpetgeo.2013.11.003.

Sanz, P.F., Dasari, G.R., 2010. Controls on in-situ stress around salt bodies. 44th U.S. Rock Mechanics Symposium and 5th U.S.-Canadian Rock Mechanics Symposium, Salt Lake City.

Saura, E., Ardèvol i Oró, L., Teixell, A., Vergés, J., 2016. Rising and falling diapirs, shifting depocenters, and flap overturning in the Cretaceous Sopeira and Sant Gervàs subbasins (Ribagorça Basin, southern Pyrenees). Tectonics 35. doi:10.1002/2015TC004001.

Saura, E., Vergés, J., Martín-Martín, J.D., Messager, G., Moragas, M., Razin, P., Grélaud, C., Joussiaume, R., Malaval, M., Homke, S., Hunt, D.W., 2014. Syn- to post-rift diapirism and minibasins of the Central High Atlas (Morocco): the changing face of a mountain belt. J. Geol. Soc. 171, 97-105. doi:10.1144/jgs2013-079.

Savin, G.N., 1961. Stress Concentration around Holes: International Series of Monographs in Aeronautics and Astronautics. Pergamon Press, New York. doi:10.1017/S0368393100075854

Schachl, E., 1987. Exkursion G – Kali- und Steinsalzbergwerk Niedersachsen-Riedel der Kali und Salz AG, Schachtanlage Riedel: Zechsteinstratigraphie und Innenbau des Salzstocks von Wathlingen-Hänigsen. In Kulick, J., Paul, J. (Eds.), Exkursionsführer I – Zechsteinsalinare und Bohrkernausstellungen. International Symposium Zechstein, Wiesbaden, 69-100.

Schléder, Z., Urai, J.L., 2005. Microstructural evolution of deformation-modified primary halite from the Middle Triassic Röt Formation at Hengelo, The Netherlands. Int. J. Earth Sci. 94, 941-956. doi:10.1007/s00531-005-0503-2.

Schléder, Z., Urai, J.L., 2007. Deformation and recrystallization mechanisms in mylonitic shear zones in naturally deformed extrusive Eocene-Oligocene rocksalt from Eyvanekey plateau and Garmsar hills (central Iran). J. Struct. Geol. 29, 241-255. doi:10.1016/j.jsg.2006.08.014.

Schmeling, H., Cruden, A., Marquart, G., 1988. Finite deformation in and around a fluid sphere moving through a viscous medium: implications for diapiric ascent. Tectonophysics 149, 17-34. doi:10.1016/0040-1951(88)90116-3.

Schultz-Ela, D.D., 2003. Origin of drag folds bordering salt diapirs. AAPG Bull. 87, 757-780. doi:10.1306/12200201093.

Schultz-Ela, D.D., Jackson, M.P.A., Vendeville, B.C., 1993. Mechanics of active salt diapirism. Tectonophysics 228, 275-312. doi:10.1016/0040-1951(93)90345-K.

Schuster, D.C., 1995. Deformation of allochthonous salt and evolution of related salt-structural systems, eastern Louisiana Gulf Coast. In: Jackson, M.P.A., Roberts, D.G., Snelson, S. (Eds.), Salt Tectonics: a Global Perspective. AAPG Mem. 65, 177-198. doi:10.1306/M65604C8.

Smith, A.P., Fischer, M.P., Evans, M.A., 2012. Fracture-controlled palaeohydrology of a secondary salt weld, La Popa Basin, NE Mexico. In: Alsop, G.I., Archer, S.G., Hartley, A.J., Grant, N.T., Hodgkinson, R. (Eds.), Salt Tectonics, Sediments and Prospectivity. Geol. Soc. Spec. Pub. 363, 107-130. doi:10.1144/SP363.6.

Snidero, M., Muñoz, J.A., Carrera, N., Butillé, M., Mencos, J., Motamedi, H., Piryaei, A., Sàbat, F., 2019. Temporal evolution of the Darmadan salt diapir, eastern Fars region, Iran. Tectonophysics 766, 115-130. doi:10.1016/j.tecto.2019.06.006.

Spiers, C.J., Carter, N.L., 1998. Microphysics of rocksalt flow in nature. In: Aubertin, M., Hardy, H.R. (Eds.), The Mechanical Behavior of Salt: Proceedings of the 4th Conference, Series on Rock and Soil Mechanics 22. Trans Tech Publ., Clausthal-Zellerfeld, 115-128.

Stewart, S.A., 2006. Implications of passive salt diapir kinematics for reservoir segmentation by radial and concentric faults. Mar. Pet. Geol. 23, 843-853. doi:10.1016/j.marpetgeo.2006.04.001.

Stovba, S.M., Stephenson, R.A., 2002. Style and timing of salt tectonics in the Dnieper-Donets Basin (Ukraine): implications for triggering and driving mechanisms of salt movement in sedimentary basins. Mar. Pet. Geol. 19, 1169-1189. doi:10.1016/S0264-8172(03)00023-0.
Thompson Jobe, J.A., Giles, K.A., Hearon, T.E. IV, Rowan, M.G., Trudgill, B., Gannaway Dalton, C.E., Jobe, Z.R., 2019. Controls on the structural and stratigraphic evolution of the megaflap-bearing Sinbad Valley salt wall, NE Paradox Basin, SW Colorado. Geosphere 16. doi:10.1130/GES02089.1.
Trudgill, B.D., Rowan, M.G., 2004. Integrating 3D seismic data with structural restorations to elucidate the evolution of a stepped counter-regional salt system, eastern Louisiana shelf, northern Gulf of Mexico. In: Davies, R.J., Cartwright, J.A., Stewart, S.A., Lappin, M., Underhill, J.R. (Eds.), 3D Seismic Technology: Applications to the Exploration of Sedimentary Basins. Geol. Soc., London, Mem. 29, 165-176. doi:10.1144/GSL.MEM.2004.029.01.16.
Trusheim, F., 1960. Mechanism of salt migration in northern Germany. AAPG Bull. 44, 1519-1540. doi:10.1306/0BDA61CA-16BD-11D7-8645000102C1865D.
Tvedt, A.B.M., Rotevatn, A., Jackson, C.A.-L., 2016. Supra-salt normal fault growth during the rise and fall of a diapir: perspectives from 3D seismic reflection data, Norwegian North Sea. J. Struct. Geol. 91, 1-26. doi:10.1016/j.jsg.2016.08.001.
Urai, J.L., Schléder, Z., Spiers, C.J., Kukla, P.A., 2008. Flow and transport properties of salt rocks. In: Littke, R., Bayer, U., Gajewski, D. Nelskamp, S. (Eds.), Dynamics of Complex Intracontinental Basins: The Central European Basin System. Springer, Berlin, 277-290.
Veatch, A.C., 1899. The five islands, Louisiana State Experimental Stations. Geol. Agriculture, 259-260.
Vendeville, B.C., Jackson, M.P.A., 1992. The rise of diapirs during thin-skinned extension. Mar. Pet. Geol. 9, 331-353. doi:10.1016/0264-8172(92)90047-I.
Vendeville, B.C., Nilsen, K.T., 1995. Episodic growth of salt diapirs driven by horizontal shortening. In: Travis, C.J., Harrison, H., Hudec, M.R., Vendeville, B.C., Peel, F.J., Perkins, B.F. (Eds.), Salt, Sediment, and Hydrocarbons: 16th Annual GCSSEPM Foundation Bob F. Perkins Res. Conf., 285-295. doi:10.5724/gcs.95.16.0285.
Waldron, J.W.F., Barr, S.M., Park, A.F., White, C.E., Hibbard, J., 2015. Late Paleozoic strike-slip faults in Maritime Canada and their role in the reconfiguration of the northern Appalachian orogen. Tectonics 34. doi:10.1002/2015TC003882.
Wallace, W.E., 1944. Structure of South Louisiana deep-seated domes. AAPG Bull. 28, 1249-1312. doi:10.1306/3D9336B0-16B1-11D7-8645000102C1865D.
Warren, J.K., 2016. Evaporites – a Geological Compendium, 2nd Ed. Springer, Cham.
Warsitzka, M., Kley, J., Kukowski, N., 2013. Salt diapirism driven by differential loading – some insights from analogue modelling. Tectonophysics 591, 83-97. doi:10.1016/j.tecto.2011.11.018.
Weijermars, R., Jackson, M.P.A., Vendeville, B.C., 1993. Rheological and tectonic modeling of salt tectonic provinces. Tectonophysics 217, 143-174. doi:10.1016/0040-1951(93)90208-2.
Wilkins, S., Mount, V., Butaud, T., Lindsey, B., Adiguna, H., Syrek, J., Fenn, C., Matthews, I., Davies, R., 2019. Subseismic deformation in traps adjacent to salt stocks/walls: observations from Green Canyon, Gulf of Mexico. In: Fiduk, J.C., Mount, V., Hearon, T.E. IV (Eds.), Salt Tectonics, Associated Processes, and Exploration Potential: Revisited 1989-2019. GCSSEPM Foundation Perkins-Rosen Research Conference, 357-364.
Williams, N.J., Fischer, M.P., Canova, D.P., 2019. Structural evolution and deformation near a tertiary salt weld, Willouran Ranges, South Australia. Mar. Pet. Geol. 102, 305-320. doi:10.1016/j.marpetgeo.2018.12.035.
Willson, S.M., Fredrich, J.T., 2005. Geomechanics considerations for through- and near-salt well design. Soc. Pet. Eng., SPE 95621. SPE Annual Technical Conference and Exhibition. doi:10.2118/95621-MS.
Withjack, M.O., Scheiner, C., 1982. Fault patterns associated with domes – an experimental and analytical study. AAPG Bull. 66, 302-316. doi:10.1306/03B59AFD-16D1-11D7-8645000102C1865D.
Worrall, D.M., Snelson, S., 1989. Evolution of the northern Gulf of Mexico, with an emphasis on Cenozoic growth faulting and the role of salt. In: Bally, A.W., Palmer, A.R. (Eds.), The Geology of North America – an Overview. The Geology of North America, v. A. Geol. Soc. Am., Boulder, 97-138. doi:10.1130/DNAG-GNA-A.97.

Wu, Z., Yin, H., Wang, X., Zhao, B., Zheng, J., Wang, X., Wang, W., 2015. The structural styles and formation mechanism of salt structures in the southern Precaspian Basin: insights from seismic data and analog modeling. Mar. Pet. Geol. 62, 58-76. doi:10.1016/j.marpetgeo.2015.01.010.
Yin, H., Groshong, R.H. Jr., 2007. A three-dimensional kinematic model for the deformation above an active diapir. AAPG Bull. 91, 343-363. doi:10.1306/10240606034.
Yin, H., Zhang, J., Meng, L., Liu, Y., Xu, S., 2009. Discrete element modeling of the faulting in the sedimentary cover above an active salt diapir. J. Struct. Geol. 31, 989-995. doi:10.1016/j.jsg.2008.10.007.
Yu, Z., Lerche, I., Lowrie, A., 1991. Modeling fracturing and faulting within sediments around rapidly moving lateral salt sheets. AAPG Bull. 75, 1772-1778. doi:10.1306/0C9B2A01-1710-11D7-8645000102C1865D.